Neurotoxicity Research (2023) 41:408–430
https://doi.org/10.1007/s12640-023-00648-1

RESEARCH

In Silico Interactions of Natural and Synthetic Compounds with Key Proteins Involved in Alzheimer's Disease: Prospects for Designing New Therapeutics Compound

Mehran Ebrahimi Shah-abadi[1] · Armin Ariaei[2] · Fatemeh Moradi[3] · Auob Rustamzadeh[3] · Rastegar Rahmani Tanha[4] · Nader Sadigh[5] · Mohsen Marzban[6] · Mahdi Heydari[3] · Vahid Tavakolian Ferdousie[7]

Received: 23 November 2022 / Revised: 26 December 2022 / Accepted: 16 April 2023 / Published online: 22 April 2023

Abstract

Memory impairment is a result of multiple factors including amyloid-beta (Aβ) accumulation. Several receptors are mediated for Aβ transport and signaling. Moreover, blood lipids are involved in Aβ signaling pathway through these receptors. Mediated blood lipid level by statins aims to regulate Aβ signaling cascade. First, the structure of receptors was taken from the RCSB PDB database and prepared with MGLTools and AutoDock tool 4. Second, the ligand was prepared for docking through AutoDock Vina. The binding affinity was calculated, and the binding sites were determined through LigPlot+ software. Besides, pharmacokinetic properties were calculated through multiple software. Finally, a molecular dynamics (MD) simulation was conducted to evaluate ligands stability along with clustering analysis to evaluate proteins connection. Our molecular docking and dynamic analyses revealed silymarin as a potential inhibitor of acetylcholinesterase (AChE), P-glycoprotein, and angiotensin-converting enzyme 2 (ACE2) with 0.704, 0.85, and 0.83 Å for RMSD along with -114.27, -107.44, and -122.51 kcal/mol for free binding energy, respectively. Moreover, rosuvastatin and quercetin have more stability compared to silymarin and donepezil in complex with P-glycoprotein and ACE2, respectively. Eventually, based on clustering and pharmacokinetics analysis, silymarin, rosuvastatin, and quercetin are suggested to be involved in peripheral clearance of Aβ. The bioactivity effects of mentioned statins and antioxidants are predicted to be helpful in treating memory impairment in Alzheimer's disease (AD). Nevertheless, mentioned drug effect could be improved by nanoparticles to facilitate penetration of the blood–brain barrier (BBB).

Keywords Peripheral dyslipidemia · Pharmacokinetics · Alzheimer's disease · Amyloid beta · Bioinformatics

✉ Auob Rustamzadeh
auob2020rustamzade@gmail.com

1 Department of Surgery, Afzalipour Hospital, Kerman University of Medical Sciences, Kerman, Iran

2 Student Research Committee, Faculty of Medicine, Iran University of Medical Sciences, Tehran, Iran

3 Department of Anatomy, School of Medicine, Iran University of Medical Sciences, Tehran, Iran

4 Department of Neurosurgery, School of Medicine, Imam Reza Hospital, Kermanshah University of Medical Sciences, Kermanshah, Iran

5 Department of Emergency Medicine, Trauma and Injury Research Center, School of Medicine, Iran University of Medical Sciences, Tehran, Iran

6 Student Research Committee, Iranshahr University of Medical Sciences, Iranshahr, Iran

7 Department of Neurosurgery, Bahonar Hospital, Kerman University of Medical Sciences, Kerman, Iran

Introduction

Amyloid-β (Aβ) is the trigger of the devastative and progressive procedure of Alzheimer's disease (AD) pathological cascade as a prominent neurodegeneration disease (Chiu et al. 2015). Aβ transport and metabolism are two aspects of the clearance pathway involved in diminishing the toxicity impact. In the transporting aspect, low-density lipoprotein receptor-related protein 1 (LRP1) and receptor for advanced glycation end-products (RAGE) have two contradicting functions in the blood–brain barrier (BBB), in which LRP1 participates in the efflux of Aβ from interstitial fluid (Cai et al. 2018). LRP1, in addition to transporting, has multiple functions for which its deletion causes early embryonic lethality (Shinohara et al. 2017). In contrast, RAGE inhibition has not depicted any fatality in the case of inhibition, thus becoming a candidate target for developing novel AD medications (Cui

et al. 2017). Above all, P-glycoprotein (P-gp) is highlighted as a modulator of AB-level in the BBB (Mohamed et al. 2016). In addition to the Aβ transporting aspect, it is worth mentioning β-site amyloid precursor protein cleaving enzyme 1 (BACE1), which involves in the amyloidogenic pathological pathway (Huang et al. 2020). Furthermore, angiotensin-converting enzyme 2 (ACE2), unlike mentioned proteins, its function has yet to be discovered. ACE2 with a wide range of expression among cells, even in astrocytes and microglia, is downregulated in the hippocampus and middle frontal gyrus (Cui et al. 2021) and conceptualized to be correlated with AD, more specifically with the level of Aβ and phosphorylated tau (p-tau) (Mawuenyega et al. 2010).

It is sophisticated to link Aβ toxicity with dyslipidemia, even though an increasing number of documents have been compiled in regard to the role of cholesterol in the accumulation of Aβ plaques (Mori et al. 2001). In animal research, hypercholesterolemic rabbits had an increased amount of Aβ1–42 deposition in the cortex and hippocampus (Jin et al. 2018). The current theories suggest the involvement of blood lipids with inflammatory cytokines, including IL-1 and TNF-α, in the disruption of the BBB and molecular cascades resulting in neural apoptosis. Accordingly, in the Yang et al.'s study, the high level of cerebral triglycerides (TG) was associated with an enhancement in IL-1, TNF-α, FFA, ox-LDL, Aβ, VEGF, GFAP, and apoptosis of neurons (Yang et al. 2017). Notably, inflammation in AD can occur as the result of Aβ accumulation, or even the reverse of this in which interleukin (IL)-6 and IL-1β as a product of activated microglia and astrocytes soar the expression of amyloid-beta precursor protein (APP) and eventually enhance Aβ deposition. Thus, the role of statins and antioxidants is highlighted in altering amyloidogenesis pathways indirectly through adjusting blood lipids and inflammation or directly by modulating Aβ receptors (Mirzaei et al. 2022).

Besides, natural statins and antioxidants have multiple pleiotropic effects, such as acting as promoting angiogenesis and neurogenesis, protecting cortical neurons from excitotoxicity, and preventing ischemic stroke. Moreover, they have direct and indirect anti-inflammatory and immunomodulatory effects in inducing pro-inflammatory responses (Banfi et al. 2017; Bhat et al. 2021; Husain et al. 2019). For instance, rosuvastatin administration has been found to significantly reduce NF-κB expression (Husain et al. 2017). Likewise, silymarin discloses a protective effect against oxidative stress. Silymarin is mainly derived from milk thistle with the main isoforms name silybin (synonym to silibinin, including silybin A and silybin B) (Soleimani et al. 2019). Moreover, its neuroprotective effect is highlighted in managing elevated levels of free radicals, nitrite content, and inflammatory mediators (Borah et al. 2013).

In silico tools such as molecular docking and dynamics help researchers to assess molecular interaction at the atomic scale as a cost-efficient alternative to complicated lab tests (Shiri et al. 2019). Moreover, analyzing the behavior of ligands in complex with targeted proteins over time could be simulated with high details in molecular dynamics (Dege et al. 2022). In this regard, in silico tools have a promising role in predicting the pharmacokinetics and pharmacodynamics of novel medications (Gökce et al. 2022). Furthermore, calculating the binding affinity of the ligands' interactions with targeted proteins and estimating drug-likeness scores is useful in drug development (Jagadeb et al. 2019; Malathi et al. 2019).

The exact mechanism of action of statins and antioxidants in the amyloidogenesis pathway has not been completely discovered. Therefore, in this study, first, we select statins and antioxidants, which their impact on attenuating AD symptoms has been justified by in vivo experiments; second, we assess the interaction between selected ligands with a number of receptors, enzymes and proteins that are conceptualized to be involved in AD. Moreover, memantine and donepezil participated in the analysis as the control drugs to be compared with selected ligands.

Methods

The current study explores the binding pattern of atorvastatin, donepezil, silymarin, memantine, quercetin, and rosuvastatin against their target proteins, listed as follows: LRP, Amyloid fibril, MRP1, RAGE, Human Amyloid Precursor Like Protein1, Aβ 1_42 monomer/pentamer, Aβ 1_40 monomer, Aβ 1_42 fibril, BACE1, acetylcholinesterase (AChE), Human Amyloid Precursor Like Protein2, ABCA1, Glial fibrillary acidic protein (GFAP), ACE2, NMDA receptor, TNF α, P-tau from AD brain, and P-glycoprotein. In addition, we describe the pharmacokinetic properties of these ligands.

Receptor Structure Information and Preparation

All protein files were downloaded from the RCSB PDB database (https://www.rcsb.org) and all the PDB ID were listed in Table 1 (Table 1). All the proteins encoded by *Homo sapiens* genes and the latest and the most appropriate ones were selected. Subsequently, protein files were prepared by MGLTools and AutoDock tool 4 (Morris et al. 2009; Sanner 1999) as follows: bond orders were automatically assigned, and atoms were systemically adjusted to the AutoDock atoms types. Water molecules were eliminated and polar hydrogen was added to the molecules. Finally, Gasteiger-Marsili charges were added to the molecules and saved in PDBQT format for docking.

Table 1 Grid box property

Proteins	PDB ID	Grid points			Grid spacing (Å)	Center points		
		X (Å)	*Y* (Å)	*Z* (Å)		*X*	*Y*	*Z*
Low-density lipoprotein receptor-related protein (LRP)	1I0U	126	38	28	1	1.397	-1.418	-1.528
Amyloid fibril (synthesis)	2BFI	26	26	100	1	2.206	7.499	22.079
Multi-drug resistance-associated protein 1 (MRP1)	2CBZ	40	40	40	1	-12.779	50.904	14.912
Receptor for advanced glycation end products (RAGE)	3O3U	126	90	86	1	26.035	17.800	72.738
Human Amyloid Precursor Like Protein1	3PMR	110	78	28	1	24.598	-31.698	20.653
Aβ 1_42 monomer	1Z0Q	54	30	30	1	-1.733	1.693	-6.759
Aβ 1_42 pentamer	2BEG	48	26	30	1	-1.816	1.582	-9.267
Aβ 1_40 monomer	2LFM	28	46	36	1	3.598	-2.106	-17.421
Aβ 1_42 fibril	2MPZ	64	76	100	1	137.007	-37.816	109.357
Interleukin 6 (IL-6)	4ZS7	40	40	40	1	29.895	58.427	20.194
Beta-secretase 1 (BACE1)	5DQC	40	40	40	1	-3.853	-24.183	28.912
Acetylcholinesterase (AChE)	5HF6	40	40	40	1	1.308	-64.520	-24.885
Human Amyloid Precursor Like Protein2	5TPT	48	66	46	1	1.821	-3.490	8.242
ATP-binding cassette transporter (ABCA1)	5XJY	100	66	112	1	127.338	133.543	131.685
Glial fibrillary acidic protein (GFAP)	6A9P	40	118	40	1	-2.363	-257.128	776.221
Angiotensin-converting enzyme 2 (ACE2)	6 M18	100	32	82	1	162.822	182.684	215.206
N-methyl-D-aspartate (NMDA) receptor	7EOQ	40	40	40	1	131.819	131.844	140.328
Tumor necrosis factor alpha (TNF-α)	7JRA	40	40	40	1	-6.717	-1.716	-29.488
P-tau from AD brain	7MKF	82	62	18	1	159.654	163.452	154.304
P-glycoprotein	7O9W	52	60	58	1	159.733	156.651	133.348

Binding Pocket Selection and Generation of Grid Box for Docking Studies

Grid box prediction for docking studies was generated using AutoDock Tools 4.2. There was blind docking and it was an attempt to adjust the grid box in a way to completely cover most of the center amino acids of the protein. Grid box spacing was as follows (Table 1).

Ligand Preparation

PubChem database was used for downloading the 3D structure of ligands atorvastatin, donepezil, silymarin, memantine, quercetin, and rosuvastatin (Table 2). Each ligand was downloaded in SDF format. Then, open babel software was used to convert SDF to PDB (O'Boyle et al. 2011) (https://openbabel.org/). Subsequently, each ligand was prepared as follows: Gasteiger charges were applied, non-polar hydrogen bonds were merged, aromatic carbons and rotatable bonds were detected, and finally, TORSDOF was set and the file saved in PDBQT format.

Molecular Docking

For performing molecular docking, AutoDock Vina was used (Trott and Olson 2010). The energy range and exhaustiveness were set at four and eight as a default, respectively.

Hit Compound Optimization

Some of the bioactive and natural compounds may interact with various types of molecules and make a false positive response (Dahlin et al. 2015). To cope with this problem searching for these compounds which are known as PAINS (pan assay interference) was performed by false positive remover software (http://cbligand.org/PAINS/search_struct.php). After checking, none of our ligands has this property. Toxicity and drug-likeness of ligands were checked through Osiris property explorer (Sander 2001) with the following address (http://www.cheminfo.org/Chemistry/Cheminformatics/Property_explorer/index.html). Moreover, the evaluation ligands for Lipinski's rule of five following database was used (https://chemicalize.com).

Table 2 Ligand properties

	Atorvastatin	Donepezil	Silymarin	Memantine	Quercetin	Rosuvastatin
PubChem ID	60823	3152	71590100	4054	5280343	75292442

Some important pharmacokinetic properties of ligands classified by absorption, distribution, metabolism, and excretion were predicted using pkCSM software (Pires et al. 2015) (http://biosig.unimelb.edu.au/pkcsm).

Visual Presentations

To draw the 3D structure of proteins in bond with ligands, Mgltool and AutoDock were used. To visualize amino acids of the proteins in bond with ligand and the type of bonds, LigPlot+ software was utilized with the academic license of Iran University of Medical Sciences (Laskowski and Swindells 2011).

Molecular Dynamic Simulation

Finally, for ligands with the highest binding affinity to target proteins, we conduct a molecular dynamics (MD) simulation with the aid of NAMD 2. NAMD was chosen because it is CPU and GPU analysis basis and has high-performance simulations (Phillips et al. 2020). First, the most suitable conformation of ligand in binding with protein calculated by AutoDock Vina was isolated to perform MD. Second, the ligand topography file was generated via CHARMM-GUI (Jo et al. 2008; Kim et al. 2017), and the topography file of the target protein was calculated automatically by VMD software (Humphrey et al. 1996). The ligand and protein subsequently were placed inside a solvent box with a 0.15 molar ion to better simulate in vivo conditions. The number of steps calculated for MD was 50,000,000 which is equal to 100 ns plus 1000 step energy minimization as the default MD setting, except for p-gp and ACE2 with 50 ns simulation due to its high number of atoms. Eventually, the output file was saved every 50,000 steps (Pasieka et al. 2021). Root mean square fluctuation (RMSF) and root mean square deviation (RMSD) measurements were calculated and visualized on the plot by VMDICE (Knapp et al. 2010). VMD installed extension was utilized for the calculation of the number of hydrogen bonds. Free binding energy as an indicator of all intermolecular interactions was calculated by the CaFE tool (Liu and Hou 2016).

Clustering Analysis

In this study, the connection between mentioned proteins was analyzed by Cytoscape software (https://www.cytoscape.org) (Shannon et al. 2003). The data for the proteins connection was derived from the STRING database consisting of proteins' interaction as well as two values of string text-mining and string score (Szklarczyk et al. 2015). The betweenness centrality was analyzed with Cytoscape software, while the closeness centrality was determined by the following formula:

Table 3 Binding affinity (kcal/mol) of ligands and proteins in the best conformation

Protein	Binding affinity (kcal/mol)					
	Atorvastatin	Donepezil	Silymarin	Memantine	Quercetin	Rosuvastatin
p-tau from AD brain	-5.2	-5.5	-6.1	-3.9	-5.1	-5.4
Amyloid fibril (synthesis)	-4.9	-5.2	-4.6	-3.7	-4.2	-4.3
Aβ 1_42 monomer	-5.8	-6.2	-6.9	-4.8	-6.0	-6.0
Aβ 1_42 pentamer	-6.4	-7.2	-6.5	-4.7	-5.7	-6.3
Aβ 1_40 monomer	-5.8	-7.0	-7.9*	-5.2	-6.7	-6.3
Aβ 1_42 fibril	-6.9	-7.0	-7.7*	-4.8	-6.3	-6.7
LRP-1	-5.8	-6.2	-6.2	-4.5	-6.0	-5.3
MRP1	-6.9	-6.8	-7.5	-5.5	-6.9	-6.4
RAGE	-7.3	-8.4*	-9.1**	-6.5	-8.1*	-6.9
p-Glycoprotein	-8.9*	-8.8*	-9.1**	-6.2	-8.4*	-8.4*
ABCA1	-7.0	-8.1*	-9.3**	-6.4	-7.7	-7.0
Amyloid precursors like protein 1	-5.9	-7.0	-7.4	-6.1	-7.0	-6.9
IL-6	-6.4	-7.2	-7.2	-5.2	-6.5	-6.5
Acetylcholinesterase (AChE)	-7.6	-8.4*	-8.8*	-7.5	-10.5**	-8.1*
Amyloid precursors like protein 2	-7.4	-7.3	-8.3*	-5.4	-7.5	-6.3
GFAP	-5.8	-5.5	-5.8	-4.4	-5.8	-5.7
ACE2	-7.8*	-7.9*	-8.4*	-5.9	-7.8*	-7.1
TNF-α	-7.5	-9.6**	-8.7*	-6.9	-8.7*	-9.6**
BACE1	-6.2	-6.8	-7.0	-4.9	-6.7	-6.7
NMDA receptor	-7.4	-7.2	-8.4*	-5.6	-6.7	-7.6

*Fairly high binding affinity; **High binding affinity ($\Delta G_{bind} \leq$ -9 kcal/mol)

Table 4 Toxicity risk of compounds and drug likeness

	Atorvastatin	Donepezil	Silymarin	Memantine	Quercetin	Rosuvastatin
Mutagenic	Low	Low	Low	Low	High	Low
Tumorigenic	Low	Low	Low	Low	High	Low
Irritant	Low	Low	Low	Low	Low	Low
Reproductive effect	High	Low	Low	Low	Low	Low
Lipinski's rule of five	No	Yes	Yes	Yes	Yes	Yes
Drug likeness	4.04	7.29	-1.34	-0.8	1.6	-1.02
Drug score	0.15	0.63	0.27	0.6	0.3	0.3

$$CC(i) = \frac{N-1}{\sum_j d(i,j)}$$

n is the number of nodes, and CC is the closeness centrality

Theory

The aim of this study was to explore whether statins and antioxidants can bind with key receptors associated with AD pathways, which might be a possible mechanism of action of these drugs for the modulation of AD pathways.

In this study, we evaluate the inhibition effect of specific AD medicine with lipid-lowering and some antioxidant medicine in silico with the aid of molecular docking, dynamics, and clustering. In this case, we could analyze the influence of lipid-lowering drugs on the signaling pathways of AD.

Results

Protein Docking

Protein docking results taken from AutoDock Vina software are presented in Table 3. As data revealed, the binding affinity of Silymarin is higher than other presented ligands to RAGE protein. This result suggests the high potential inhibitory attribute of silymarin to RAGE. Nevertheless, other ligands, donepezil and quercetin, have a rather high binding affinity for RAGE. Acetylcholinesterase (AChE), one of the major enzymes that interfere in the AD pathway, can be inhibited efficiently by quercetin. Moreover, donepezil, silymarin, and rosuvastatin can also inhibit this enzyme. Among ligands presented in this study, silymarin has the highest number of enzyme inhibition in comparison with AD common medications and other statins. P-glycoprotein can be inhibited by almost all the ligands presented in this study. In addition, N-methyl-D-aspartate (NMDA) receptor is predicted to be inhibited by silymarin. Nevertheless, by visualizing the binding site, it can be concluded that all ligands presented in this study, except for memantine has a different binding site that influences only the external part of the receptor. The data revealed that only memantine could bind to the middle of the channel efficiently in a way in which the influx of ions is interrupted (Table 3).

Predicting Pharmacologic Properties

In current study, we used the OSIRIS Property Explorer web server to predict molecular properties and other drug-associated factors of the statins in comparison with common AD. First, the toxicity potential of the presented ligands was measured. As data suggests, all the ligands are safe from a toxicity perspective except for two of them, named quercetin

Table 5 Pharmacokinetic properties

	Atorvastatin	Donepezil	Silymarin	Memantine	Quercetin	Rosuvastatin
Water solubility numeric (log mol/L)	-4.531	-4.648	-2.935	-2.317	-2.925	-5.752
Intestinal absorption (human) numeric (% absorbed)	59.861	93.707	17.277	91.234	77.207	97.036
P-glycoprotein substrate categorical (yes/no)	Yes	Yes	Yes	No	Yes	No
VDss (human) numeric (log L/kg)	-1.918	1.266	0.042	0.988	1.559	-0.329
BBB permeability numeric (log BB)	-1.162	0.157	-1.942	0.603	-1.098	-1.237
CNS permeability numeric (log PS)	-2.916	-1.464	-4.098	-2.478	-3.065	-3.075
Total clearance numeric (log ml/min/kg)	0.437	0.987	-0.269	0.548	0.407	0.738
AMES toxicity categorical (yes/no)	No	No	No	No	No	No
Max. tolerated dose (human) numeric (log mg/kg/day)	0.193	-0.217	0.453	0.322	0.499	0.642
Hepatotoxicity categorical (yes/no)	Yes	Yes	No	No	No	Yes
Skin sensitization categorical (yes/no)	No	No	No	Yes	No	No

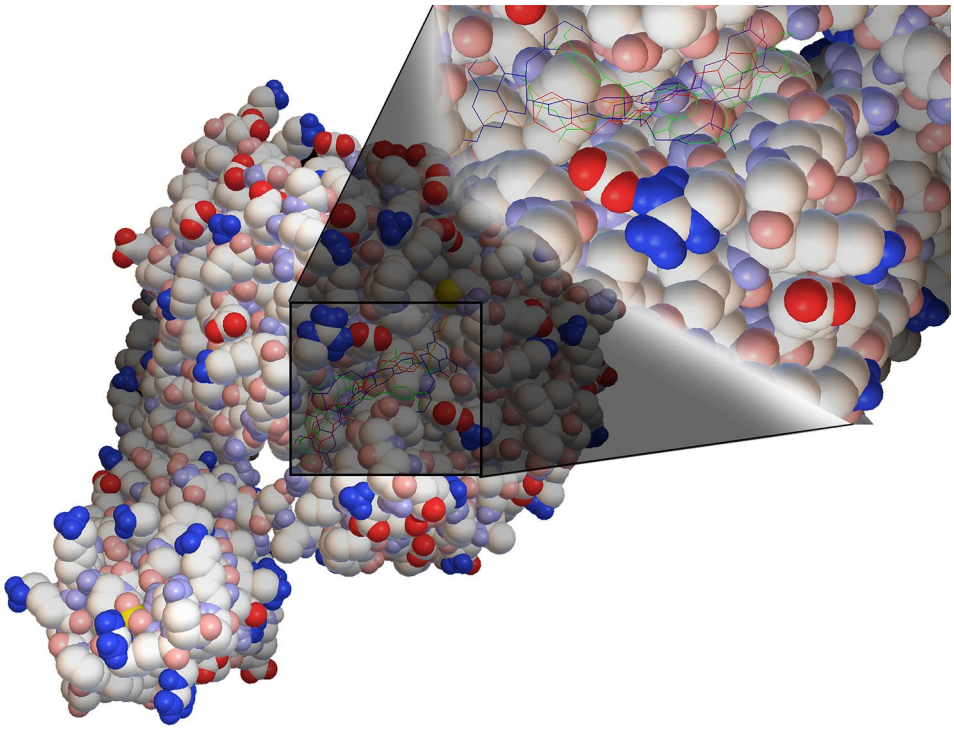

Fig. 1 RAGE 3D modeling with its inhibitor compounds. Blue, red, and white represent the positive, negative, and hydrophobic regions, respectively, while regions marked as yellow represent less negative areas. Mode1: donepezil -8.4 kcal/mol = > orange. Mode2: donepezil -8.3 kcal/mol = > red. Mode1: silymarin -9.1 kcal/mol = > blue. Mode2: silymarin -8.8 kcal/mol = > green. Mode1: quercetin -8.1 kcal/mol = > purple

and atorvastatin. In addition, atorvastatin is predicted to be harmful to the reproductive system. To measure the best way for using these drugs (oral or intravenous), we use Lipinski's rule of five. The data clearly indicated that all of them can be prescribed orally, except atorvastatin. Drug likeness and drug score are two variables to measure the quality of the drugs made by these ligands. Data suggested donepezil as the best option for drug synthesis and memantine as a second priority for drug choice. Among them, silymarin has the least drug likeness and atorvastatin has the lowest drug score (Table 4).

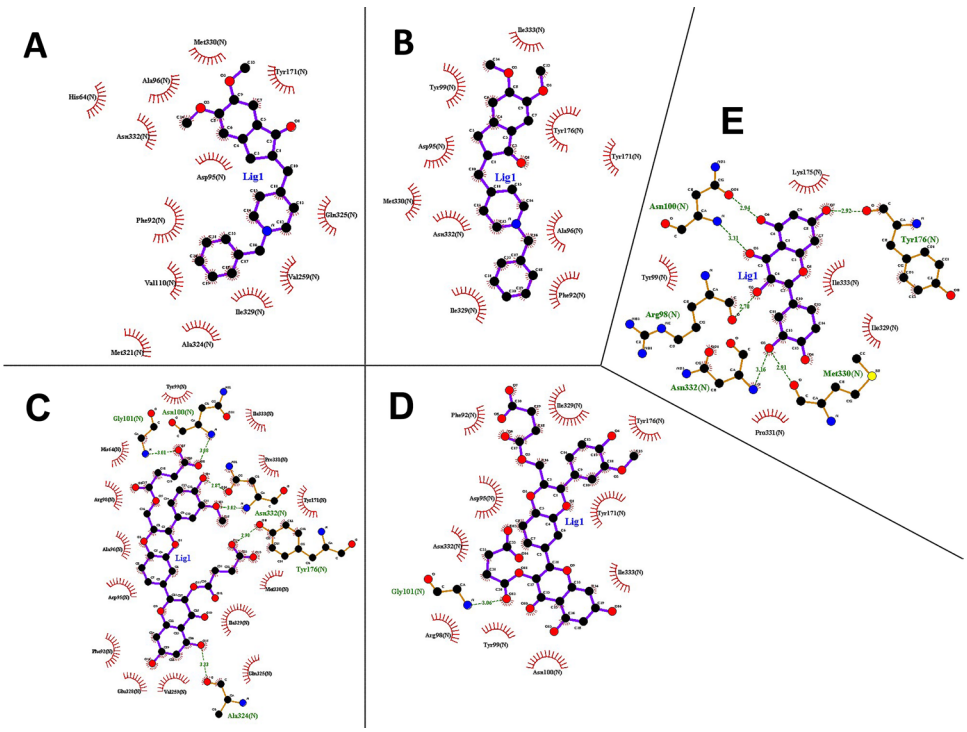

Fig. 2 The image represents the bonds ligands with RAGE. **A** Bonds of donepezil at mode1 interaction with RAGE. **B** Bonds of donepezil at mode2 interaction with RAGE. **C** bonds of at silymarin mode1 interaction with RAGE. **D** Silymarin mode2 interaction with RAGE. **E** bonds of quercetin at mode1 interaction with RAGE. The red color represent hydrophobic bonds and the green color represents hydrophobic bonds

Pharmacokinetic Property

Next, we evaluate the pharmacokinetic properties of ligands and listed important items. The result of the study depicted that memantine has the highest water solubility, while rosuvastatin has the highest tendency for lipid-solving. Silymarin has the least intestinal absorption, while other drugs have good absorption through the intestine. Only memantine and rosuvastatin cannot be p-glycoprotein substrates. Quercetin has the highest distribution in the human body. Donepezil and memantine can easily pass through the blood–brain barrier and quickly distribute in the central nervous system. Donepezil has the highest clearance rate. None of the ligands mentioned in this study has a positive AMES toxicity test. Rosuvastatin can be admitted in higher doses compared with other ligands. Silymarin, memantine, and quercetin are safe from hepatotoxicity. Finally, memantine can cause skin sensitivity (Table 5).

Binding Sites

We analyzed the binding site of protein amino acids with ligand as well as the type of bands with LigPlot+ software. TNF-α and Aβ 1_42 fibril were excluded from binding site analysis because ligands bind to the core of the proteins, and their conformation changes are hard to be predicted. Moreover, ABCA1 has a myriad number of atoms, and mentioned ligands bind to this protein unspecifically leading to failing to find the protein active site. Similar to ABCA1, the NMDA receptor is excluded from binding site analysis, for none of the ligands has a similar binding site to memantine. Finally, in our study, Aβ 1_40 monomer was not scrutinized, since the level of this protein was not heightened in AD, and due to its non-toxicity property, it has less influence on the AD pathological signaling cascade (Tijms et al. 2018).

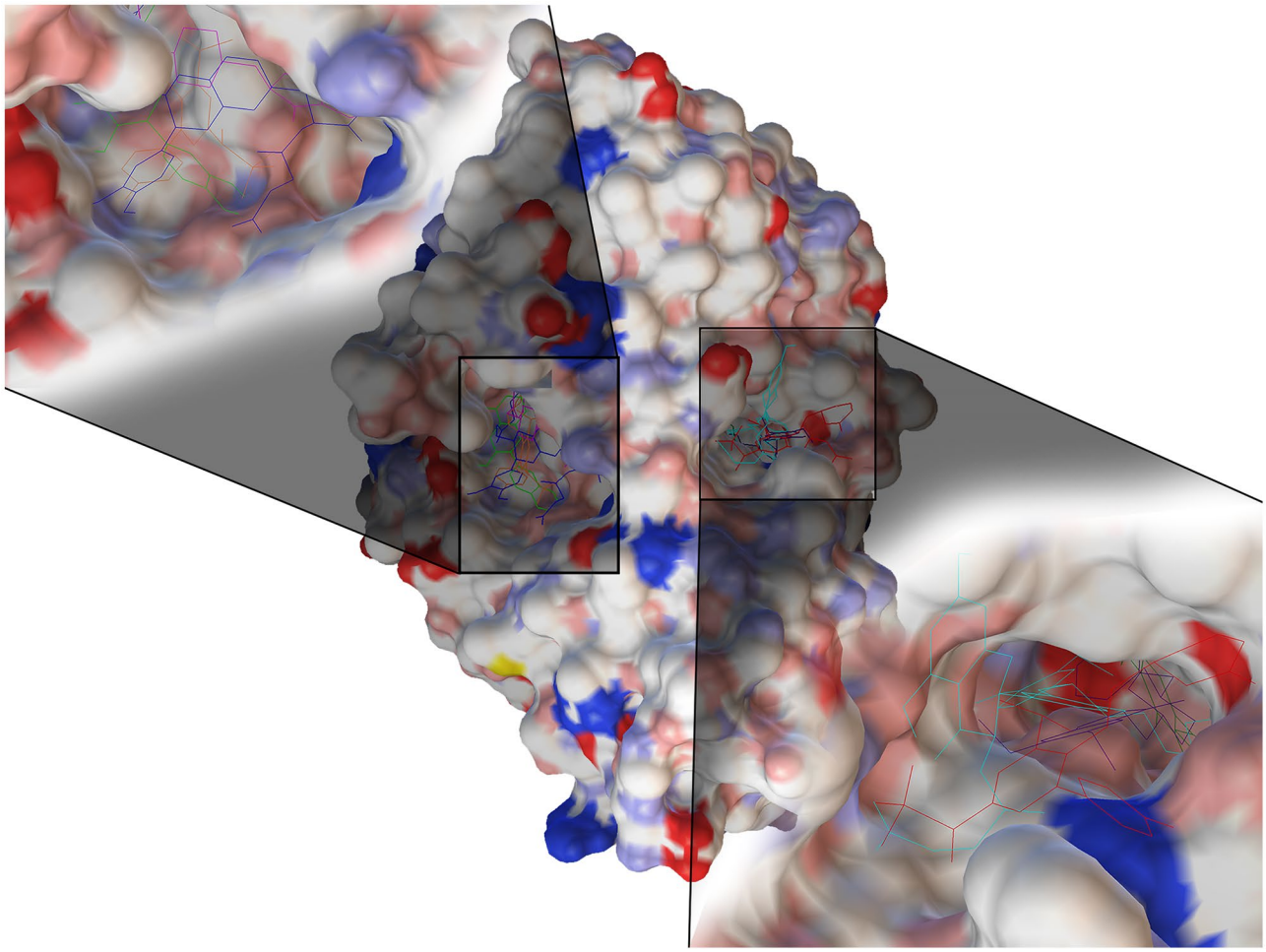

Fig. 3 Acetylcholinesterase (AChE) 3D modeling with its inhibitor compounds. Blue, red, and white represent the positive, negative, and hydrophobic regions, respectively, while regions marked as yellow represent less negative areas. Mode1: rosuvastatin = > red. Mode2: donepezil = > purple. Mode2: silymarin = > light blue. Mode 1: quercetin = > green. Mode1: donepezil = > pink. Mode1: silymarin = > blue. Mode3: rosuvastatin = > orange. Mode6: quercetin = > light green

RAGE

By analyzing the binding sites of ligands, we realized that isoleucine 329 is the crucial amino acid in involvement in ligand binding, since this amino acid participates in all five modes of ligand binding. Moreover, mode 1 silymarin has the highest number of hydrophobic and hydrophilic bonds, 14 and 5 bonds, respectively. This data is in line with the binding affinity of silymarin. Donepezil only has hydrophobic bonds, in contrast to silymarin and quercetin. Asparagine 100 is a crucial amino acid in hydrogen bonds. In addition, methionine 330 takes part in both hydrophilic and hydrophobic bonds. Phenylalanine 92, aspartic acid 95, and tyrosine 171 are involved in all ligand bonds except for quercetin (Figs. 1 and 2).

Acetylcholinesterase

Binding site analysis of acetylcholinesterase highlighted quercetin and silymarin as effective compounds for inhibiting the enzyme's activity. Silymarin makes 13 hydrophobic and 7 hydrogen bonds, while quercetin makes nine hydrophobic and seven hydrogen bonds. Since quercetin has a significantly high binding affinity, new synthesis compounds should focus on making hydrogen bonds. Effective amino acids for making these bonds are histidin 447 and 405, glutamic acid 202 and 313, asparagine 87, tyrosine 72, aspartic acid 74, serine 125, glutamine 71, threonine 311, and glycine 240. Leucine 289, proline 235, and tyrosine 72 are the crucial amino acids for ligand binding since these two amino acids participated in most of the ligand bonds. Serine 293 and aspartic acid 74 are involved in the highest number of hydrogen bonds similarity among ligands, as well as hydrophobic. Histidine 405 and phenylalanine 295 participated in both hydrogen bonds and hydrophobic bonds (Figs. 3 and 4).

Human Amyloid Precursor-Like Protein-2

Among ligands presented in this study, only silymarin has a high binding affinity for APP. The data revealed the hydrogen bond as a key bond for stable ligand–protein binding. Histidine amino acid participated in multiple hydrophobic and hydrogen bonds. Histidine 510 and 513 are similar in hydrogen bonds of both silymarin modes. All the amino acids that participated in bonds are located far from the C-terminal of protein, ranging from 383 to 568 amino acid numbers (Fig. 5).

P-glycoprotein

Analyzing binding sites revealed silymarin to have the highest number of bonds (17 bonds) among other ligands. The results derived from AutoDock Vina also justified the high tendency of silymarin to bind to P-gp. The binding sites of silymarin and atorvastatin have the highest similarity

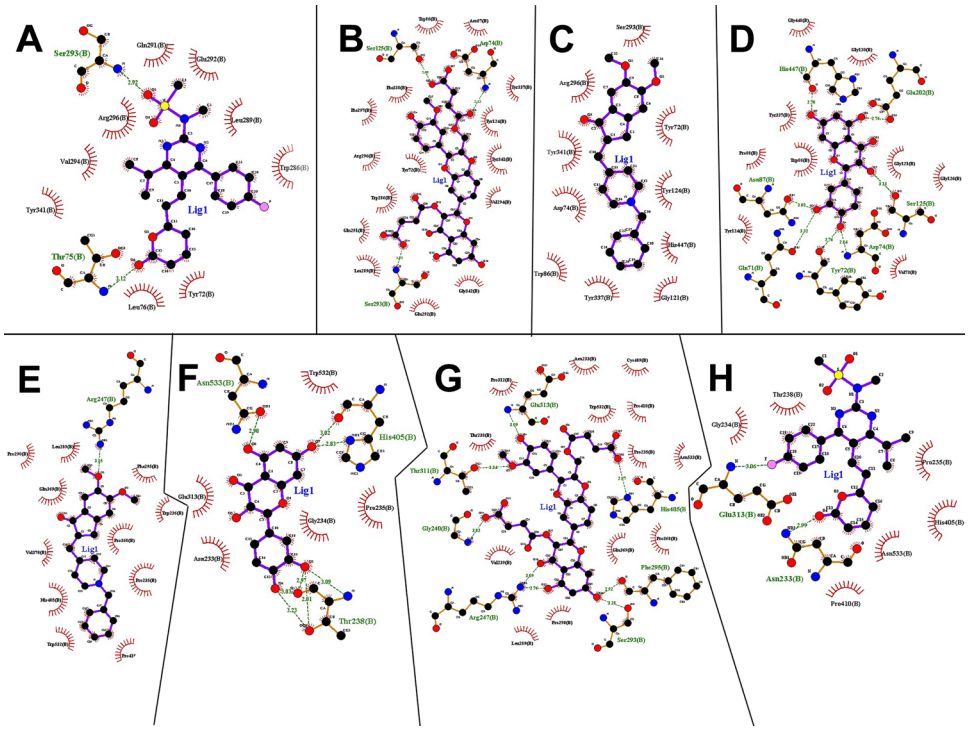

Fig. 4 The image represents the bonds ligands with AChE. **A** Bonds of rosuvastatin at mode1 interaction with AChE. **B** Bonds of silymarin at mode2 interaction with AChE. **C** Bonds of at donepezil mode2 interaction with AChE. **D** Bonds of quercetin mode1 interaction with AChE. **E** Bonds of donepezil at mode1 interaction with AChE. **F** Bonds of quercetin at mode6 interaction with AChE. **G** Bonds of silymarin at mode1 interaction with AChE. **H** Bonds of rosuvastatin at mode3 interaction with AChE. The red color represents hydrophobic bonds and the green color represents hydrophobic bonds

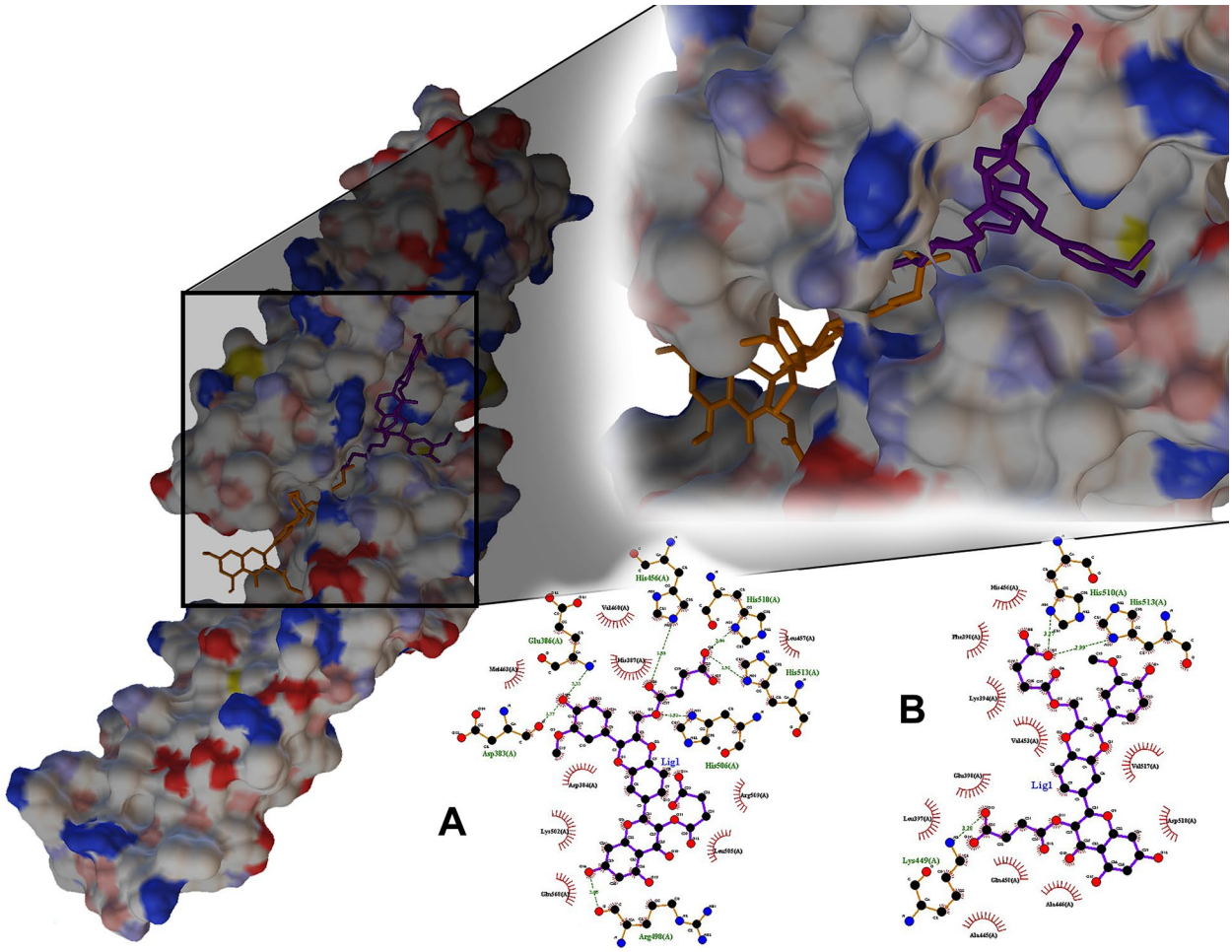

Fig. 5 3D modeling of Amyloid precursor-like protein-2 with its inhibitor compounds. Blue, red, and white represent the positive, negative, and hydrophobic regions, respectively, while regions marked as yellow represent less negative areas. Silymarin mode1 represents purple while silymarin mode2 is colored in orange. **A** Silymarin mode1. **B** Silymarin mode2

compared to other ligands with seven shared amino acids (Gly830, Gly781, Gly 827, Phe777, Gln 773, Phe770, and Ile299), while donepezil shared no amino acids in binding site with other ligands. Among amino acids that participated in hydrophobic and hydrogen bonds, Gln773 makes both hydrogen and hydrophobic bond and Phe777, Gln773, Phe770, and Gln838 are key amino acids of P-gp for ligand binding (Figs. 6 and 7).

ACE2

Binding site analysis determined silymarin as a potential compound for binding to ACE2 with 13 hydrophobic and 2 hydrogen bonds. Among amino acids, Arg482 involves in both hydrogen and hydrophobic bonds. Asp494 is the crucial amino acid since it is shared in 3 bonds of three ligands. Other necessary amino acids are listed as Val672, His493, Ala 673, Leu675, Lys 475, glu479, and 489 (Figs. 8 and 9).

MD Simulation

To better criticize and compare the inhibitory property and stability of the mentioned ligands with the common drugs of AD an MD simulation was performed. In this simulation, the protein fluctuation rate and the stability of hydrogen bonds were determined. In the MD simulation, the results for the RAGE suggested instability state of ligand and protein since the RMSD value revealed a high structural changes of 20 to 6 angstrom. Therefore, we excluded RAGE from further MD analysis.

AChE

The role of AChE in the symptoms' onset of AD is inevitable; hence, we assess all the high binding affinity ligands in complex with this enzyme. As is depicted in Fig. 10, silymarin has the highest stability in complex with AChE due to the RMSD value (overall 0.704 Å) and the number of

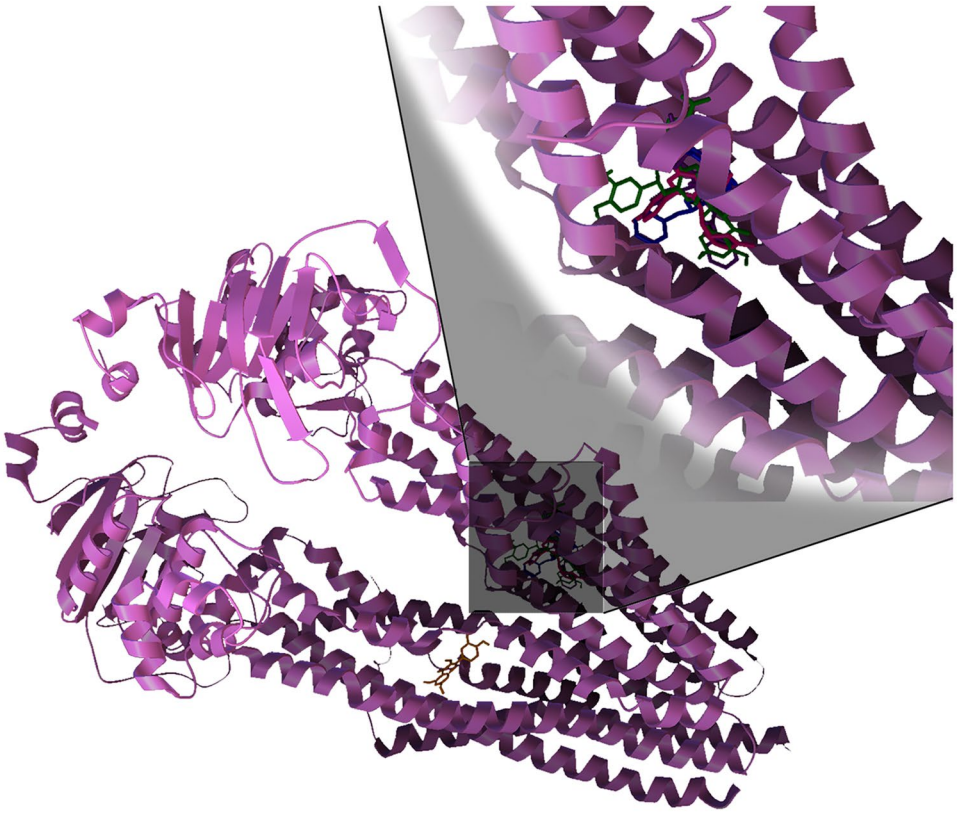

Fig. 6 P-glycoprotein 3D modeling with its inhibitor compounds. Silymarin mode1 represents green while donepezil mode2 is colored in blue. Also, mode1 rosuvastatin, quercetin, and atorvastatin are colored in pink, orange, and purple, respectively. As it was depicted, quercetin binding sites differ from other ligands

hydrogen bonds (up to 6). Nevertheless, silymarin depicted a mean value among selected ligands in the assessment of RG (fluctuating between 22.85 and 23.10 Å). In the RG parameter, rosuvastatin has the lowest RG value (mean 22.87 Å) indicating less instability in contrast to RMSD results. The RMSF value demonstrated high fluctuation in four range of residues (130–200, 240–290, 353, and 420), which is illustrated the involvement of these residues in ligand binding. Donepezil and silymarin have more impact on AChE residues compared to quercetin and rosuvastatin. In consequence, due to the RG and hydrogen bond results, rosuvastatin and quercetin depicted rather more stability in complex with AChE compared to donepezil (Fig. 10). To better assess ligands binding strength, the free binding energy was compared between these four ligands, which the results are presented in Table 6. Besides, quercetin has the highest number of hydrogen bonds, which cause the complex more stable and the electrostatic contribution (-44.21 kcal/mol) become superior to all listed ligands in complex with AChE (Table 6).

P-glycoprotein

Since P-gp has a substantial number of amino acids, all-atom MD simulation is hard to be implemented for a prolonged period. For this and the following protein, the MD simulation was performed with 50 ns. Among ligands with high binding affinity, quercetin had a different binding site compared to other ligands; thus, it was excluded from MD simulation due to its less possibility to influence the enzyme's active site. In the RMSD, there were no significant differences between selected lipid-lowing ligands and donepezil with an overall value of 0.85, 0.826, 0.858, and 0.862 for silymarin, donepezil, atorvastatin, and rosuvastatin, respectively. The RMSF value suggests that donepezil and atorvastatin have a higher influence on p-gp residues, especially in the 200th residue for atorvastatin and the 623rd residue for donepezil. Silymarin demonstrated a slight instability status in RG value compared to donepezil, in contrast to the number of hydrogen bonds, which is much higher in silymarin (Fig. 11). Moreover, rosuvastatin has the highest stability in the complex due to its RG value (around 36.9 to 37 Å). Similar to silymarin, both atorvastatin and rosuvastatin depicted a higher number of hydrogen bonds (up to 4) in comparison to donepezil. Eventually, free binding energy predicted higher stability of atorvastatin (-90.3945 kcal/mol) compared to rosuvastatin (-81.6019 kcal/mol), but lower stability compared to silymarin (-107.4424 kcal/mol). These results are mainly due to the powerful hydrogen bonds between ligands and complexes, in which atorvastatin and silymarin depicted a high occupancy rate of hydrogen bonds compared to donepezil and rosuvastatin. Moreover, the MMPBSA/MMGBSA results signify

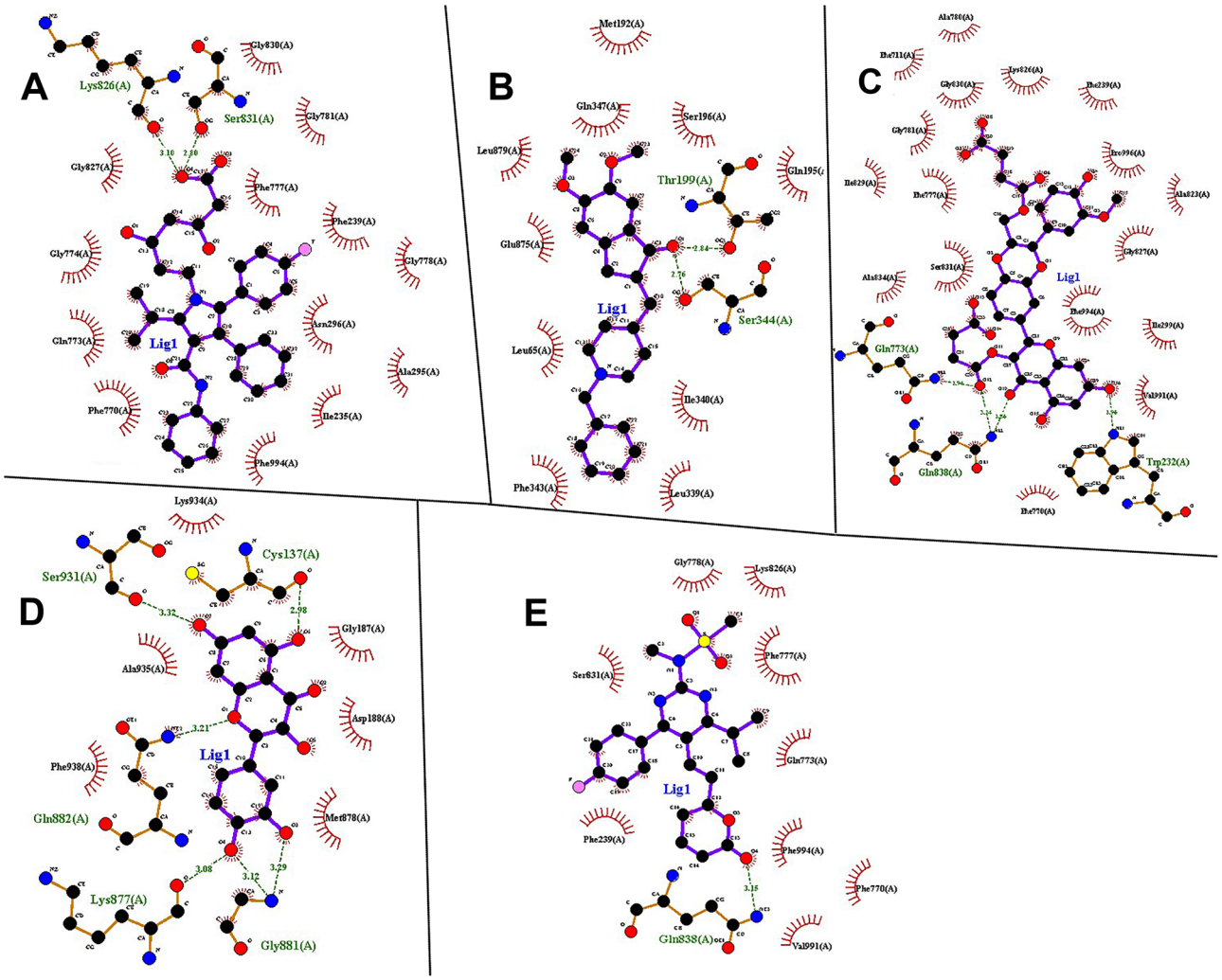

Fig. 7 The image represents the bonds ligands with P-gp. **A** Bonds of atorvastatin at mode1 interaction with P-gp. **B** Bonds of donepezil at mode1 interaction with P-gp. **C** Bonds of at silymarin mode1 interaction with P-gp. **D** Bonds of at quercetin mode1 interaction with P-gp. **E** Bonds of at rosuvastatin mode1 interaction with P-gp

rosuvastatin and silymarin for their high electrostatic contribution (-26.94 kcal/mol for rosuvastatin, -35.29 kcal/mol for silymarin). This result justifies the RMSF for silymarin and RG values for rosuvastatin, in which they illustrated a stable state with less fluctuation (Table 6).

ACE2

Similar to P-glycoprotein, in this part, we conduct a rather short MD simulation. Among four high-binding affinity ligands based on molecular docking results, atorvastatin has been excluded from MD simulation due to different binding sites. RMSD values of quercetin, in contrast to silymarin, has more stability in complex (0.783 Å). Similarly, for RMSF value, silymarin and donepezil, unlike quercetin, have more spikes which suggest fluctuation in the position of residues due to the binding posture of the ligand. In the RG value, it could be concluded that donepezil has a higher fluctuation rate, while quercetin is in a stable mode, in addition to the high number of hydrogen bonds (up to 4). Finally, the MMPBSA/MMGBSA results specified silymarin with high binding energy in complex with ACE2 (-122.5117 kcal/mol). Moreover, the number of hydrogen bonds in quercetin and silymarin complex is more than donepezil, which can be also concluded from electrostatic contribution (-58.32 kcal/mol for silymarin, -40.02 kcal/mol for quercetin). In addition, the results suggested that quercetin bonds to the ACE2 with hydrophilic bonds due to the van der Waals contribution (-32.58 kcal/mol) (Table 6 and Fig. 12).

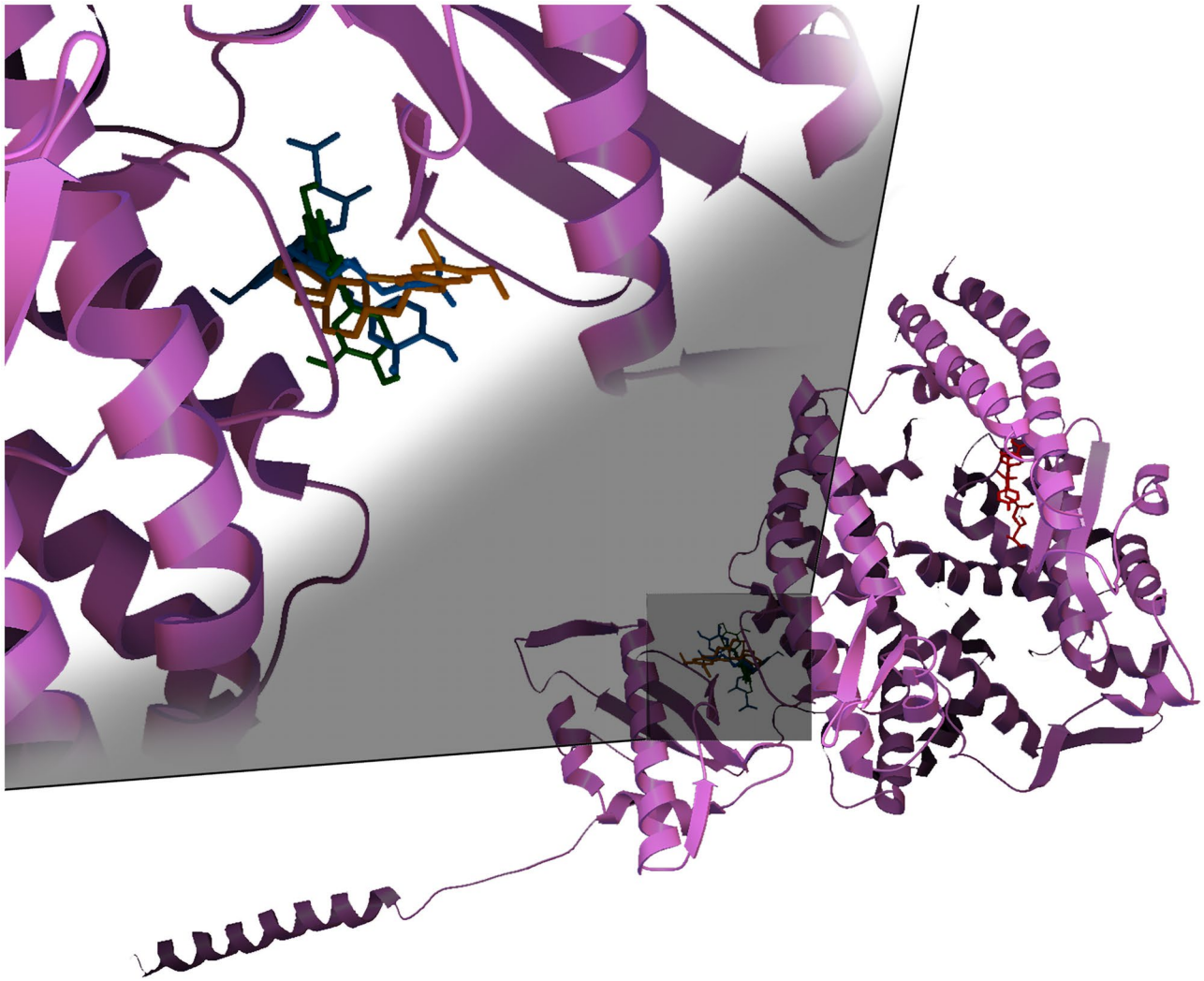

Fig. 8 ACE2 3D modeling with its inhibitor compounds. Silymarin mode1 represents blue while donepezil mode1 is colored in orange. Also, mode1 quercetin and atorvastatin are colored in green and red, respectively. As it was depicted, atorvastatin binding site differs from other ligands

Signaling Pathway

To evaluate the mentioned protein interaction and their influence on each other, in this study, protein clustering analysis was performed. The results are depicted in Fig. 13 and Table 7. One of the important parameters which help to design effective drugs to impede the pathological signaling cascade of AD is betweenness centrality. Analyzing this parameter determined the communication flow, similar to a crucial bridge, in which most of the proteins' signaling is mediated by it. Moreover, there are two other parameters named string score and string text-mining to measure how reliable is the predicted pathway. These parameters range from 0 to 1 which represent high reliability of the pathway, while a score below 0.5 indicated most probably false positive status. Based on the results, it can be indicated that IL-6 and TNF-α are the most potential candidates for drug design targeting. These results highlighted the important role of inflammation on AD. Besides the inflammation aspect, p-gp is ranked second in drug design targeting. Another parameter in protein clustering analysis is closeness centrality, in which proteins with a score near 1 are specified as having the highest communication nodes. Similar to previous results, Il-6 takes the highest score; nevertheless, the second rank is dedicated to APP which highlighted the high influence of the amyloidogenesis procedure. In this study, based on the binding affinity results and molecular dynamics, it can be concluded that mentioned lipid-lowing drugs alleviate AD symptoms by influencing the intersection aspect of lipid metabolism and amyloidogenesis signaling pathway by influencing proteins and receptors involved in both aspects, including p-gp and RAGE. Eventually, it somewhat can be concluded that these drugs can influence other aspects of AD by interacting with AChE and ACE2 proteins.

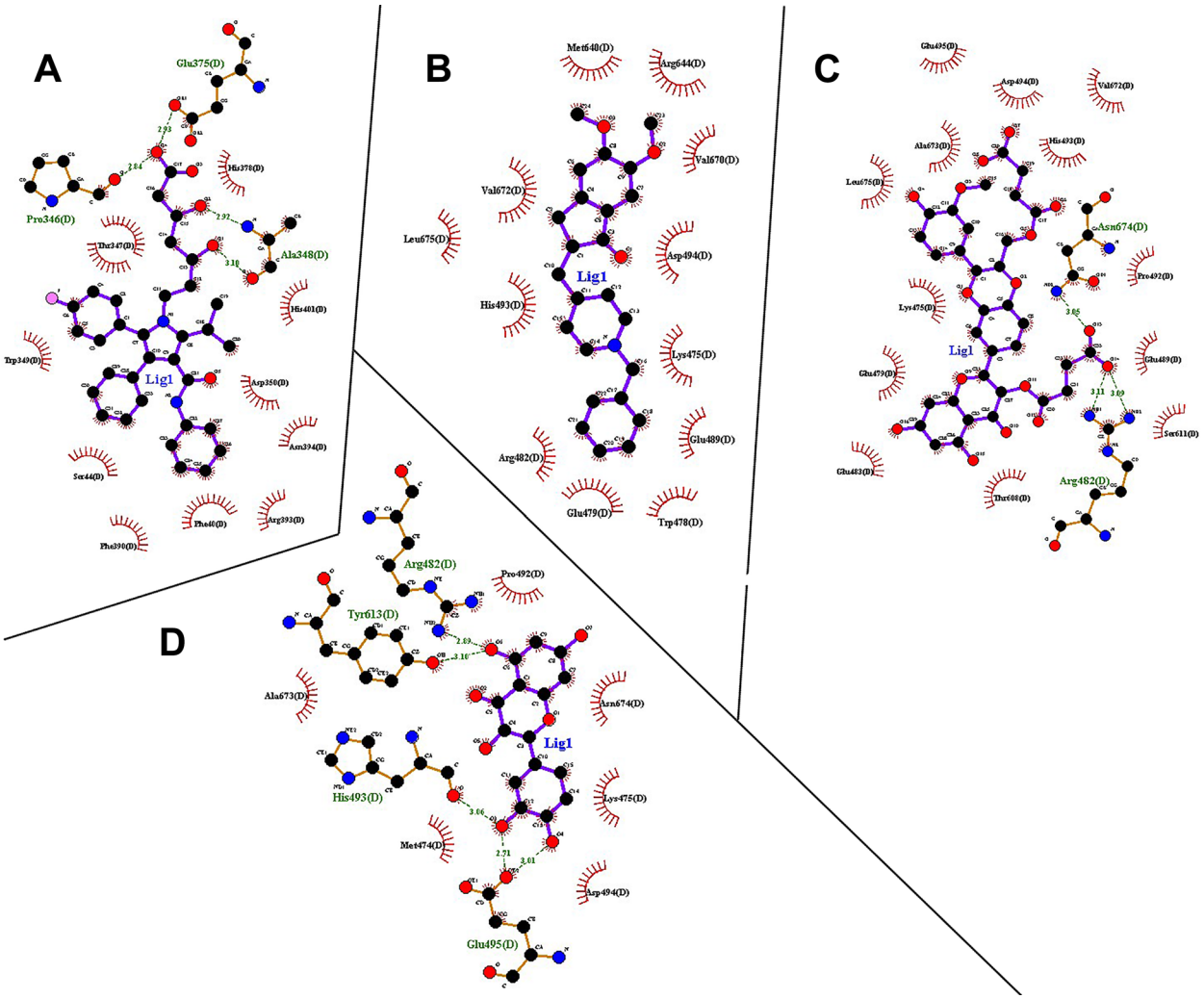

Fig. 9 The image represents the bonds ligands with ACE2. **A** Bonds of atorvastatin at mode1 interaction with ACE2. **B** Bonds of donepezil at mode1 interaction with ACE2. **C** Bonds of at silymarin mode1 interaction with ACE2. **D** Bonds of at quercetin mode1 interaction with ACE2

Discussion

In this study, we calculated the pharmacokinetics and pharmacodynamics of well-known statins and antioxidants along with two commonly used medications for AD. We aim to compare these statins' and antioxidants' properties to determine whether they have the potential to be used as an AD medication, also compare our in silico data with in vivo data derived from various articles to evaluate the validity of data extracted from in silico experiments.

Studies suggested rosuvastatin's anti-neuroinflammatory properties either in reducing microglial load or inhibiting the inflammatory cascade (Husain et al. 2018). Moreover, its interaction in reducing the production of several inflammatory factors like interleukin-10, tumor necrosis factor (TNF-α), and other compounds like nitric oxide and NF-κB in important brain areas including the CA1 region of the hippocampus is somehow unknown (Husain et al. 2017). Since the result of our study shows a high binding affinity of rosuvastatin toward TNF-α, it suggests rosuvastatin changes the conformation of TNF-α and may reduce the effects of this protein resulting in disruption of the inflammatory signaling cascade. For the pharmacokinetics of this statin, in a human study, the bioavailability of rosuvastatin has been estimated by considering its metabolism by liver enzymes concluded in a long duration of action and plasma half-life which is higher than any other statin (Toth and Dayspring 2011). This property could be due to less dependency on the CYP3A metabolism pathway (Vuorio et al. 2022). Our results are in contrast with these findings, since it is suggested rather fast total clearance through the kidney.

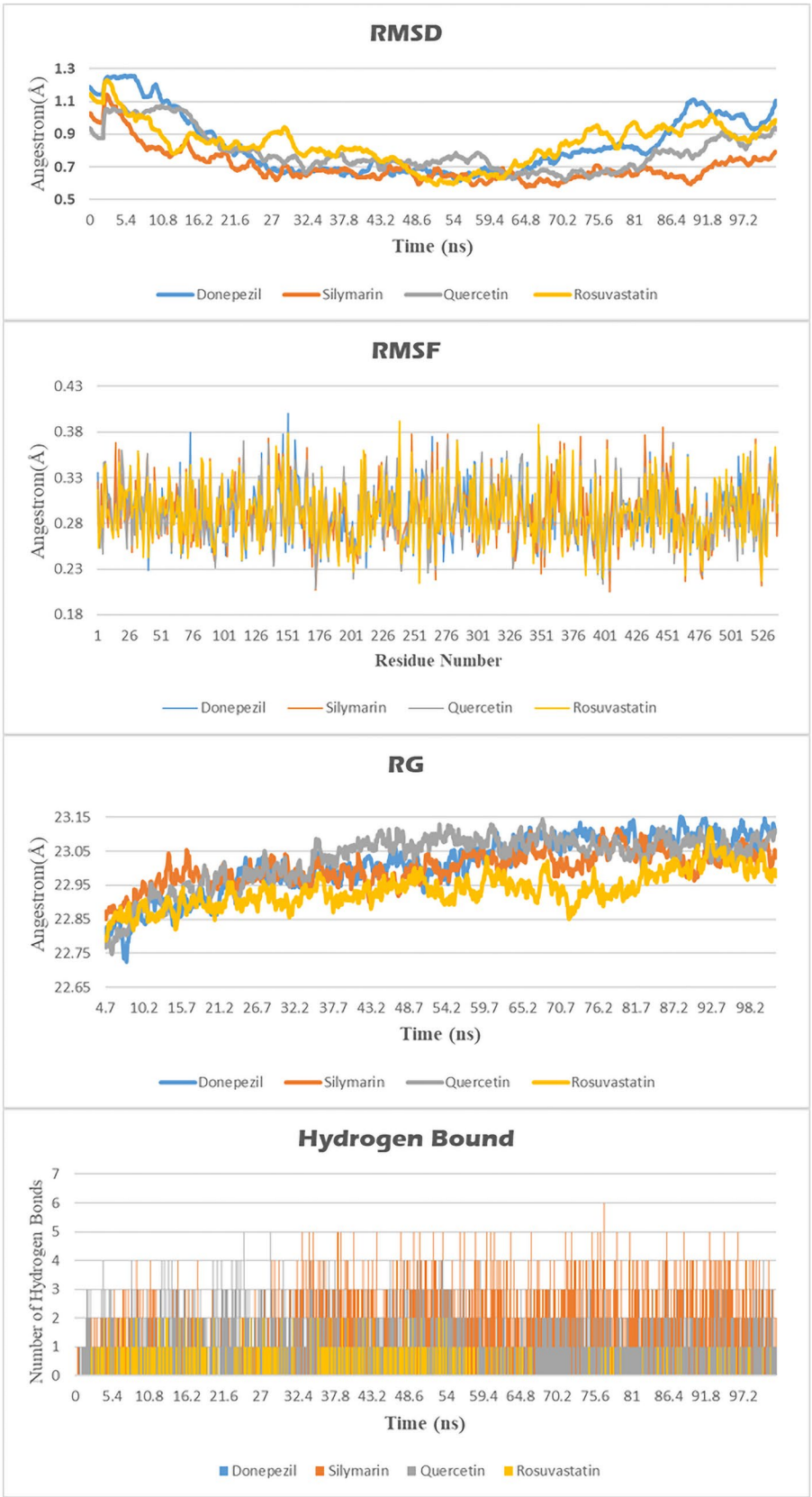

Fig. 10 RMSD, RMSF, RG, and hydrogen bounds are illustrated in the following charts. The overall value of RMSD for donepezil, silymarin, quercetin, and rosuvastatin is 0.839, 0.704, 0.792, and 0.842, respectively. The value of RMSF is calculated per residues

Table 6 Hydrogen bounds are defined in more detail with the determination of donor and acceptor hydrogen as well as their occupancy in the simulation period

Proteins	Ligands	Free binding energy (kcal/mol)		Donor	Acceptor	Occupancy
		Mean	SD			
AChE	Donepezil	ΔElec: -26.7164	6.6721	None	None	0
		ΔVdw: -50.9522	3.4229			
		ΔSA: -5.0574	0.0906			
		ΔGas: -77.6686	8.2609			
		ΔNpol: -56.0097	3.4284			
		Total: -82.7260	8.2596			
	Silymarin	ΔElec: -43.9412	7.7886	SER293	Silymarin	1.57%
		ΔVdw: -63.8847	3.7911	Silymarin	GLN291	51.71%
		ΔSA: -6.4525	0.1310	SER125	Silymarin	1.08%
		ΔGas: -107.8259	8.4143	SER293	Silymarin	30.85%
		ΔNpol: -70.3372	3.8248	TYR337	Silymarin	34.28%
		Total: -114.2783	8.4580	Silymarin	SER125	53.77%
				TYR124	Silymarin	57.79%
				Silymarin	GLU292	2.35%
	Quercetin	ΔElec: -44.2181	7.0206	Quercetin	GLU202	35.36%
		ΔVdw: -38.6112	3.0553	Quercetin	SER125	26.74%
		ΔSA: -3.4058	0.0685	Quercetin	TYR72	11.56%
		ΔGas: -82.8293	6.0253	Quercetin	HSD447	28.40%
		ΔNpol: -42.0170	3.0568	Quercetin	GLY448	25.56%
		Total: -86.2351	6.0266	Quercetin	ASP74	0.49%
				TYR124	Quercetin	3.92%
				TYR133	Quercetin	3.72%
				Quercetin	ASN87	7.64%
				ASP74	Quercetin	3.92%
				TYR337	Quercetin	0.20%
				Quercetin	TRP86	1.27%
	Rosuvastatin	ΔElec: -14.9889	7.1431	THR75	Rosuvastatin	19.10%
		ΔVdw: -37.0501	2.6684	TYR72	Rosuvastatin	7.54%
		ΔSA: -4.0671	0.1915	SER293	Rosuvastatin	13.52%
		ΔGas: -52.0390	8.2380	THR75	Rosuvastatin	0.10%
		ΔNpol: -41.1172	2.7661			
		Total: -56.1061	8.3841			
P-pg	Atorvastatin	ΔElec: -19.1640	4.0649	Atorvastatin	LYS826	3.85%
		ΔVdw: -64.8260	3.4536	Atorvastatin	SER831	4.62%
		ΔSA: -6.4044	0.1469	SER831	Atorvastatin	52.31%
		ΔGas: -83.9900	5.1154	GLN773	Atorvastatin	3.85%
		ΔNpol: -71.2304	3.4395	Atorvastatin	PHE777	0.19%
		Total: -90.3945	5.1057	ASN296	Atorvastatin	0.19%
	Donepezil	ΔElec: -24.4483	4.0198	SER831	Donepezil	24.21%
		ΔVdw: -43.0217	2.5597	GLN773	Donepezil	9.65%
		ΔSA: -4.7784	0.1196			
		ΔGas: -67.4700	4.3044			
		ΔNpol: -47.8001	2.6015			
		Total: -72.2484	4.2962			
	Silymarin	ΔElec: -35.2953	6.7647	Silymarin	SER831	3.65%
		ΔVdw: -65.2892	4.0226	GLN838	Silymarin	23.22%
		ΔSA: -6.8578	0.1566	SER831	Silymarin	49.90%
		ΔGas: -100.5846	8.2233	LYS826	Silymarin	0.19%
		ΔNpol: -72.1470	4.0953	Silymarin	GLN990-S	10.17%
		Total: -107.4424	8.2857	TRP232	Silymarin	9.02%
				Silymarin	GLY830-M	0.19%
				GLN773	Silymarin	0.58%
				Silymarin	PHE777-S	0.58%
				Silymarin	LYS826-M	11.52%
				ASN296	Silymarin	6.91%

Table 6 (continued)

Proteins	Ligands	Free binding energy (kcal/mol)		Donor	Acceptor	Occupancy
		Mean	SD			
	Rosuvastatin	ΔElec: -26.9405	4.7554	SER831	Rosuvastatin	22.12%
		ΔVdw: -49.4439	4.3291	GLN838	Rosuvastatin	20.96%
		ΔSA: -5.2176	0.1185	TRP232	Rosuvastatin	0.19%
		ΔGas: -76.3844	6.6304			
		ΔNpol: -54.6614	4.3360			
		Total: -81.6019	6.6318			
ACE2	Donepezil	ΔElec: -26.8706	4.3138	ARG644	Donepezil	32.82%
		ΔVdw: -48.5525	2.3621			
		ΔSA: -4.8756	0.0821			
		ΔGas: -75.4231	4.5388			
		ΔNpol: -53.4281	2.3545			
		Total: -80.2987	4.5436			
	Silymarin	ΔElec: -58.3233	10.3733	GLU479	Silymarin	0.19%
		ΔVdw: -57.9819	3.0483	LEU675	Silymarin	32.44%
		ΔSA: -6.2066	0.1093	ASN674	Silymarin	8.64%
		ΔGas: -116.3051	9.7241	ARG482	Silymarin	43.19%
		ΔNpol: -64.1884	3.0673	LYS676	Silymarin	6.33%
		Total: -122.5117	9.7635	Silymarin	ASP609	1.54%
				Silymarin	GLU479	0.19%
				SER611	Silymarin	1.73%
				Silymarin	SER611	3.84%
				Silymarin	THR608	0.19%
	Quercetin	ΔElec: -40.0223	6.6377	Quercetin	GLU495	44.04%
		ΔVdw: -32.5832	3.2176	ASN674	Quercetin	25.00%
		ΔSA: -3.4739	0.0716	Quercetin	TYR613	1.73%
		ΔGas: -72.6054	5.8049	ASN674	Quercetin	0.19%
		ΔNpol: -36.0570	3.2157	Quercetin	GLU489	11.73%
		Total: -76.0793	5.8115			

Eele electrostatic contribution, *Vdw* van der Waals contribution, *SA* solvent area, *Npol* non-polar solvation energy

Focusing on the pharmacokinetics of silymarin could conclude in high absorption in the intestine, especially in the duodenum. In contrast, the bioavailability of silymarin depicted a remarkably low value (0.95%) (Tvrdý et al. 2021). This parameter revealed less efficiency of this drug use orally. In addition, in vitro research suggested no or less water solubility of silymarin (Lee et al. 2017; Porwal et al. 2019; Schramm et al. 2018). Our results find out rather a low solubility of this component compared to water-soluble compounds like ethanol with 0.782 (log mol/L), but there is not very high lipid solubility compared to octadecenoic acids with -5.924 (log mol/L). Our results suggested that by taking 100–300 mg/kg of silymarin, the body could clear it in 3.2–9.7 h. Studies suggested six to eight hours for the clearance half-life of silymarin (Porwal et al. 2019). As it is more likely to be soluble in lipids than water, it is primarily exerted from bile, but it can be cleared via kidneys too. Other pharmacokinetic properties of this drug including BBB penetration and CNS distribution also disclose an inefficiency, since the literature suggested an amount of at least -1 for log BBB penetration and -3 for log CNS distribution (Pires et al. 2015). These results revealed a demand for nanoparticles to deliver silymarin efficiently, and these properties were confirmed by the following study. In this regard, the study put focused on nanoparticles and developed nano-liquid crystals for transporting silymarin with higher effect (Singh et al. 2020). Multiple studies measured the properties of the silymarin sub-group and report optimistic results, including impeding Aβ accumulation (Bai et al. 2019). This property could be referred to peripheral clearance of Aβ or another hypothesis known as dyslipidemia. This theory correlates the levels of HDL-C with the risk of dementia in which high HDL-C either in midlife or in late life was associated with AD pathological signs, including NFTs and Aβ plaques (Lütjohann et al. 2012). Hence, a high-fat diet could cause inflammation and synaptic plasticity loss besides cardiovascular disease (Wolozin 2011). Since statins have lipid-lowering properties, they can prevent triggering a pathological cascade of AD, which resulted in Aβ accumulation. For toxicity dose prediction, our results suggested taking about 200 mg/day of silymarin as a maximum dose for a person with 70 kg weight, which is far lower than the toxicity dosage reported by clinical trials. In a clinical trial, prescribing 100–300 mg 3 times every day in an encapsulated form of silymarin (70–80% Silymarin) had no side effects in adults. This clinical study determined

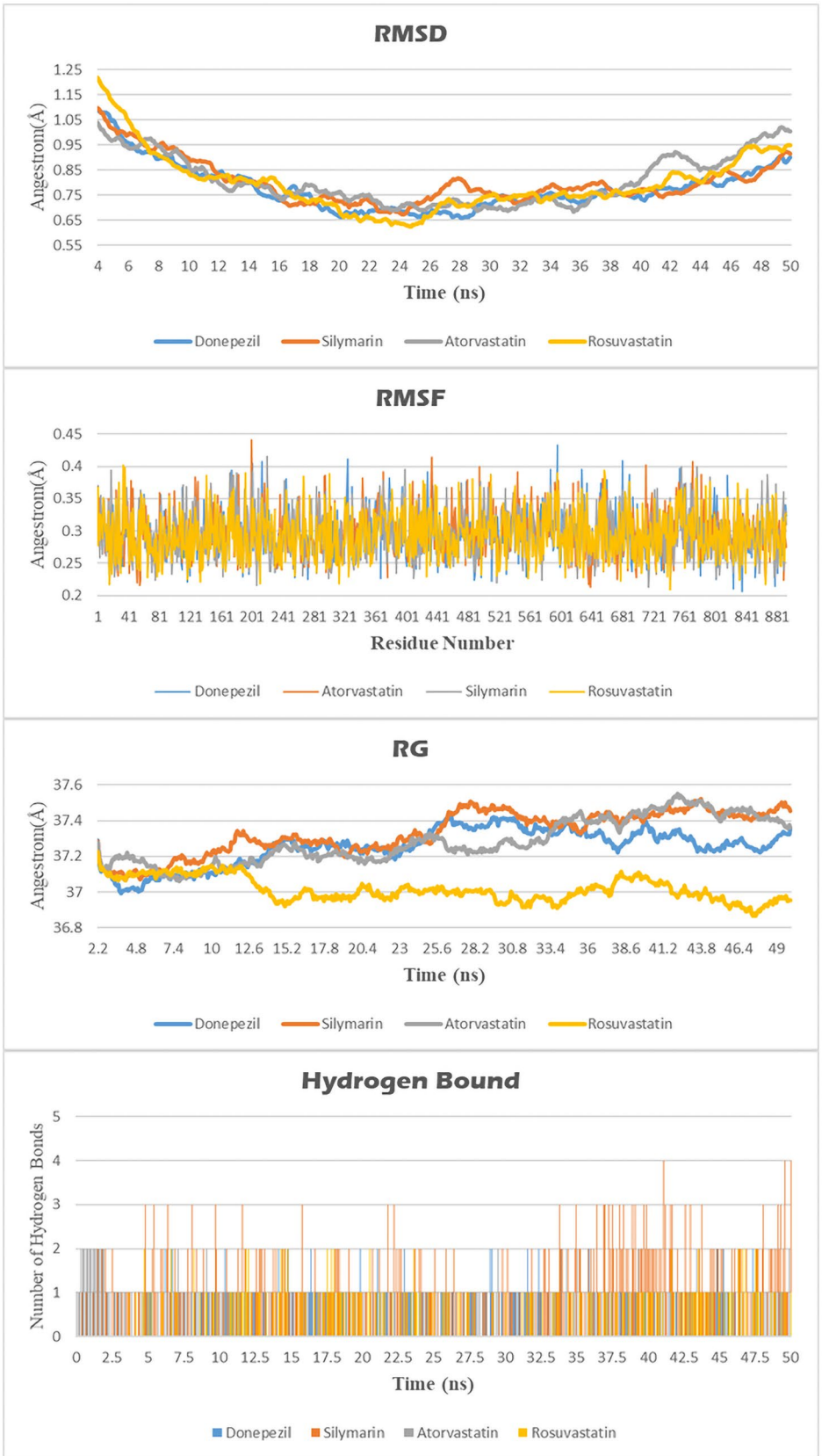

Fig. 11 RMSD, RMSF, RG, and hydrogen bound analyzed for donepezil, silymarin, atorvastatin, and rosuvastatin. The overall RMSD score was 0.858, 0.826, 0.850, and 0.862 for atorvastatin, donepezil, silymarin, and rosuvastatin, respectively

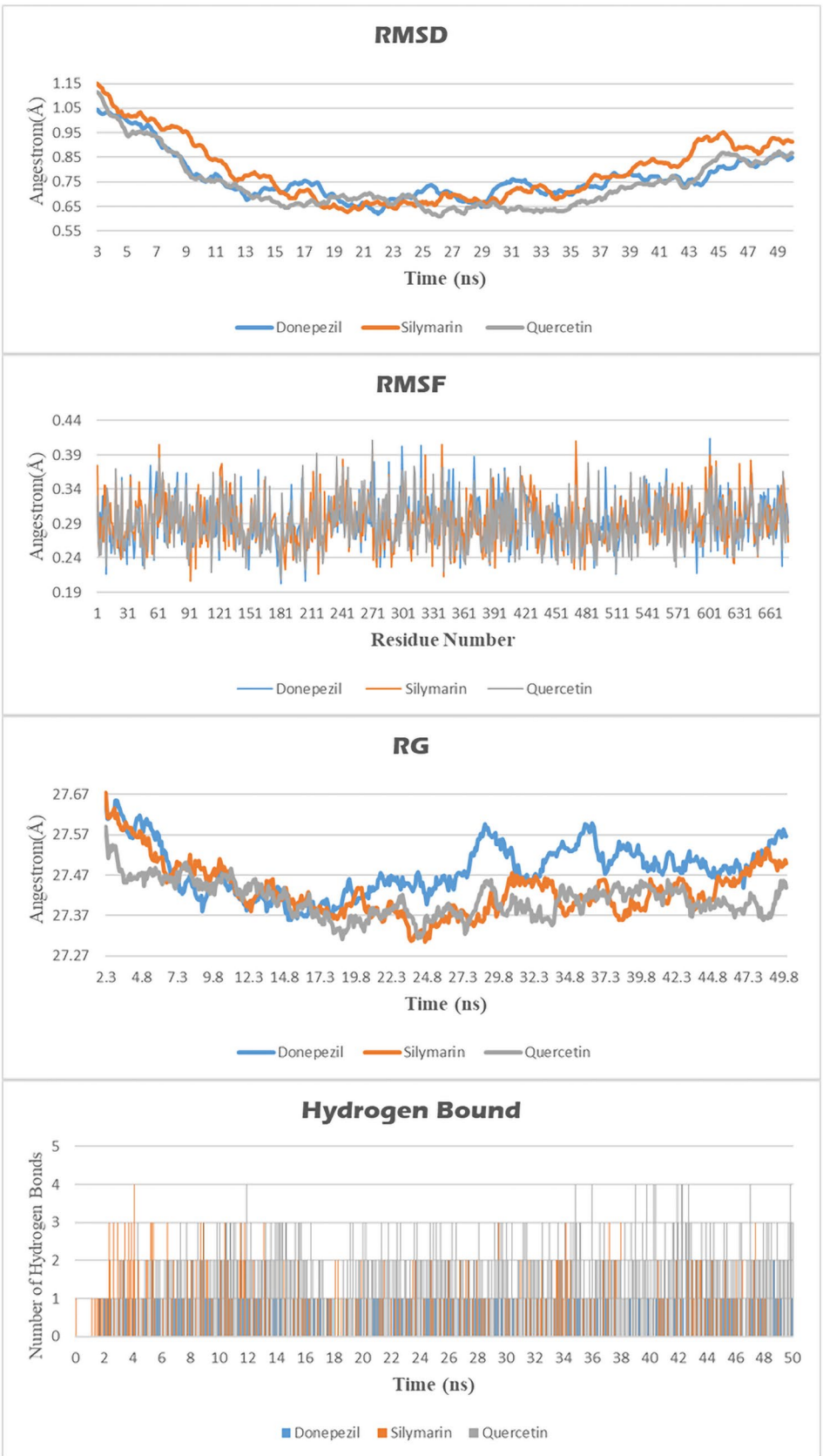

Fig. 12 RMSD, RMSF, RG, and hydrogen bound analyzed for donepezil, quercetin, and silymarin. The overall RMSD for donepezil, quercetin, and silymarin is 0.798, 0.783, and 0.833, respectively

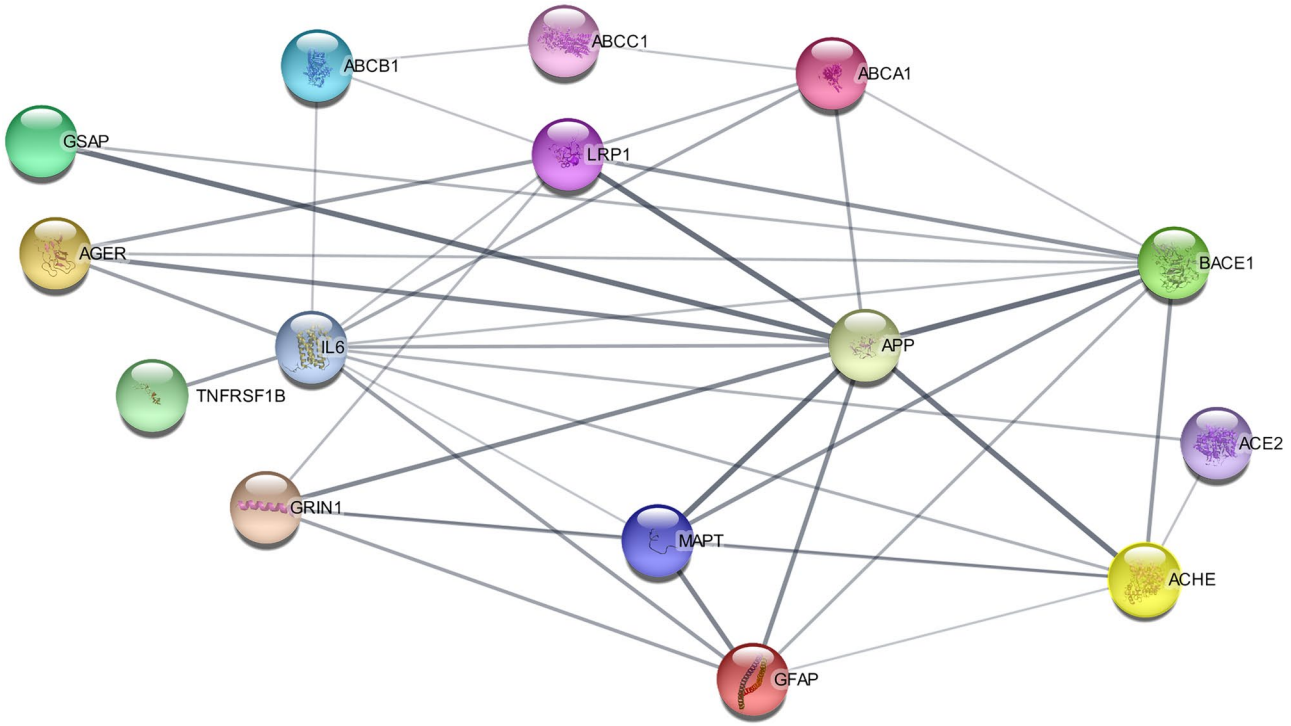

Fig. 13 Protein interaction map generated by Cytoscape software. GSAP, gamma-secretase activating protein; AGER, advanced glycosylation end product-specific receptor; MAPT, microtubule-associated protein tau; ABCC1 representation for multidrug resistance-associated protein 1 (MRP1); APP, amyloid-beta precursor protein; GRIN1 encoded Glutamate (NMDA) receptor subunit zeta-1; *AChE*, acetylcholinesterase; GFAP, glial fibrillary acidic protein; LRP, low-density lipoprotein receptor-related protein; TNFRSF1B representation for tumor necrosis factor; IL-6, interleukin 6; ACE2, angiotensin-converting enzyme 2; ABCA1, ATP-binding cassette transporter; ABCB1 representation for P-glycoprotein

1500 mg/day dosage to be known as a toxicity dose which causes high side effects mainly due to increased bile secretion and flow. Moreover, the researcher stated mild allergic reactions (Porwal et al. 2019), which are not detected by our predictions.

Our data suggested hazardous effects of atorvastatin on the reproduction system which is in line with studies conducted on rat and human which reported erectile and testicular dysfunction, altered steroid hormone production, and reducing sperms' count number (Akdeniz et al. 2020; Omolaoye et al. 2022). Also, it is worth mentioning that the mechanism of causing dysfunction in the reproduction system is remained a controversial issue since some studies stated that statins can improve the reproduction system and sperm quality (Abdulwahab et al. 2021; Davis et al. 2015; Sadeghi et al. 2021). Besides, there are several side effects reported in patients who take statins which we have not predicted. These side effects include gastrointestinal effects, myalgia and increasing creatine phosphokinase, and allergic reactions (Urina-Jassir et al. 2021).

Since statins have less BBB penetration rate, they cannot influence neurons and their products in CNS. Moreover, they have a less binding affinity toward different forms of Aβ, except for silymarin which can bind to $A\beta_{1\text{-}40}$ (not toxic) and Aβ fibril (toxic). In contrast, studies suggested administration of statins could attenuate Aβ accumulation (Bai et al. 2019; Mohamed et al. 2016). To explain this paradox, we could highlight Aβ receptors which most of the statins can bind to them efficiently. Statins strongly bind to RAGE, P-glycoprotein, ABCA1, and ACE2. These receptors interact with Aβ and are known to involve in its transport and clearance. In vitro studies conceptualize the extracellular V domain of (RAGE) as a key domain for ligand binding (Singh and Agrawal 2022; Tolstova et al. 2022; Yue et al. 2022). Our results also confirm this prediction and as depicted in Fig. 1, all compounds bind to this domain as the best confirmation (Fig. 1). However, the MD simulation contradicts these results. To explain this conflict, it is worthwhile to note that the RAGE receptor is attached to the membrane of cells. Hence, its interaction with other membrane compounds results in protein structure alternation. Therefore, since the complex system of membrane proteins is hard to simulate, in this study, just a simplified condition was simulated. ACE expressed by the endothelium and its action is mainly thought to be a mediator for salt balance. Nonetheless, its inhibition through small molecules was stated to

Table 7 Protein interaction analysis

Protein	Closeness centrality	Interaction	String text-mining	String score	Edge betweenness
LRP1	0.736	LRP1 (pp) APP	0.975	0.992	6
		LRP1 (pp) AGER	0.683	0.683	5.166667
		LRP1 (pp) GRIN1	0.383	0.48	10.03333
		LRP1 (pp) BACE1	0.674	0.747	6.4
		LRP1 (pp) IL6	0.455	0.455	8.3
		LRP1 (pp) ABCA1	0.53	0.551	6.166667
		LRP1 (pp) ABCB1	0.421	0.42	10.66667
GSAP	0.466	GSAP (pp) APP	0.941	0.969	15
		GSAP (pp) BACE1	0.516	0.516	13
APP	0.777	APP (pp) GFAP	0.709	0.793	5.333333
		APP (pp) GRIN1	0.547	0.823	7.866667
		APP (pp) BACE1	0.991	0.999	2.4
		APP (pp) AGER	0.601	0.833	6.833333
		APP (pp) ACHE	0.76	0.952	6.833333
		APP (pp) MAPT	0.883	0.969	5.333333
		APP (pp) ABCA1	0.579	0.589	12
		APP (pp) IL6	0.62	0.619	9.8
ACHE	0.636	ACHE (pp) IL6	0.537	0.536	9.633333
		ACHE (pp) ACE2	0.41	0.42	9
		ACHE (pp) MAPT	0.557	0.582	3
		ACHE (pp) BACE1	0.688	0.695	7.233333
		ACHE (pp) GRIN1	0.353	0.451	5.7
GFAP	0.608	ACHE (pp) GFAP	0.369	0.407	3
BACE1	0.736	BACE1 (pp) AGER	0.504	0.504	5.833333
		BACE1 (pp) GFAP	0.533	0.547	5.733333
		BACE1 (pp) IL6	0.468	0.468	9
		BACE1 (pp) ABCA1	0.401	0.414	10.33333
		BACE1 (pp) MAPT	0.739	0.747	5.733333
MAPT	0.608	MAPT (pp) GRIN1	0.389	0.629	3.7
		MAPT (pp) GFAP	0.568	0.845	2
		MAPT (pp) IL6	0.408	0.408	10.63333
GRIN1	0.578	GRIN1 (pp) GFAP	0.404	0.633	3.7
ABCA1	0.608	ABCA1 (pp) IL6	0.594	0.601	14
		ABCA1 (pp) ABCC1	0.334	0.425	19.83333
AGER	0.56	AGER (pp) IL6	0.661	0.661	10.16667
TNFRSF1B	0.466	TNFRSF1B (pp) IL6	0.683	0.69	28
ABCC1	0.411	ABCC1 (pp) ABCB1	0.402	0.417	9.5
IL6	0.823	IL6 (pp) GFAP	0.675	0.674	10.63333
ACE2	0.5	IL6 (pp) ACE2	0.517	0.516	19
ABCB1	0.538	IL6 (pp) ABCB1	0.42	0.419	21.5

PP protein to protein interaction

prevent Aβ aggregation (Jin et al. 2021; Le et al. 2021). Our result finds out the high binding affinity of statins to ACE2, and it may facilitate Aβ binding for peripheral clearance.

Another important finding of this study is quercetin's tumorigenic and mutagenic properties. Multiple studies declared the anti-tumor properties of quercetin and highlighted its role in eliminating tumors (Rauf et al. 2018; Reyes-Farias and Carrasco-Pozo 2019; Shafabakhsh and Asemi 2019; Tang et al. 2020). Its exact mechanism has not been clearly discovered; nevertheless, it is suggested to act through various mechanisms like regulating PI3K/Akt/mTOR, Wnt/-catenin, and MAPK/ERK1/2 pathways (Reyes-Farias and

Carrasco-Pozo 2019) or promoting cytotoxic effects. However, Shafabakhsh et al. declare that it did not affect healthy cells (Shafabakhsh and Asemi 2019), and its mutagenic properties must be assessed through various methods. Quercetin may affect cells by inducing DNA mutation, and because cancer cells have high DNA transcription, it can affect them with a higher effect than healthy cells.

Duan et al. conducted research on APP/PS1 transgenic mice with administration of 200 mg/kg silybin once a day for 28 days, and its effect was measured in vitro and in vivo. The results revealed a decline in AChE activity (Duan et al. 2015). This research outcome acknowledges our results that show silymarin and most of the statins have high binding affinity and can inhibit AChE.

As far as β-secretase known as BACE1 has a proven high impact on cleavage and metabolism of amyloid-beta precursor protein in multiple studies (Hampel et al. 2021), new biosynthesis medicine should be focused on inhibition of this enzyme. None of the compounds analyzed in our study has a high potential effect for inhibiting this enzyme. To put all the results together, our studies suggested the potential inhibitory effects of selected ligands on hallmark proteins involved in AD pathological symptoms; nevertheless, their efficiency could be improved by designing effective nanoparticles to transport and penetrate BBB, which help to increase the bioavailability of mentioned ligands in the CNS. Moreover, one of the limitations of our study is the implementation of in vitro and in vivo assessment; therefore, further in vivo and in vitro studies are needed to fully confirm the influence of the mentioned ligands on selected receptors and prove the role of statins on amyloidogenesis pathway with involvement of RAGE, ACE2, and P-gp.

Conclusion

Memory impairment as a neurological and neurophysiological phenomenon influences patients' life quality. Aβ accumulation as one of the factors which influence memory can be diminished through multiple treatment strategies. RAGE as a receptor transporting Aβ into the CNS and P-gp as a crucial mediator in Aβ signaling can be efficiently inhibited by statins as well as silymarin. AChE can be inhibited by quercetin more effectively than donepezil. In addition, statins can affect other proteins, including amyloid precursors like protein 2, ACE2, and TNF-α. The pharmacokinetic properties of statins and antioxidants reveal their ability to peripheral clearance of Aβ since they have a poor BBB penetration rate. Also, some of them (further study needed) including atorvastatin and quercetin may have a low ability to ameliorate the reproductive system failure and tumorigenicity.

Acknowledgements The authors are grateful to the research vice-chancellor of the Iran University of Medical Sciences (IUMS), Tehran, Iran. All methods and analyses were performed according to Ethics Committee instructions (IUMS Alzheimer's clinical research section) with the ethical code: IR.IUMS.FMD.REC.1400.409.

Author Contribution Auob Rustamzadeh contributed to the study's conception and design, along with writing the first draft of the manuscript and data analysis. Material preparation, figures, data collection, and analysis were performed by Armin Ariaei. Mehran Ebrahimi Shah-abadi and Fatemeh Moradi contributed to writing the first draft of the manuscript. Rastegar Rahmani Tanha, Nader Sadigh, and Mohsen Marzban contribute to writing and editing. Mahdi Heydari and Vahid Tavakolian Ferdousie contribute to reviewing. All authors commented on previous versions of the manuscript. All authors read and approved the final manuscript.

Funding This project is supported by the deputy of research at the Iran University of Medical Sciences (grant number: 20441).

Data Availability The data that support the findings of this study is openly available on the request.

Declarations

Competing Interests The authors declare no competing interests.

References

Abdulwahab DK, Ibrahim WW, Abd El-Aal RA, Abdel-Latif HA, Abdelkader NF (2021) Grape seed extract improved the fertility-enhancing effect of atorvastatin in high-fat diet-induced testicular injury in rats: involvement of antioxidant and anti-apoptotic effects. J Pharm Pharmacol 73(3):366–376

Akdeniz E, Onger ME, Bolat MS, Firat F, Gur M, Cinar O, Bakirtas M, Acıkgoz A, Erdemir F (2020) Effect of atorvastatin on spermatogenesis in rats: a stereological study. Trop J Pharm Res 19(12):2609–2614

Bai D, Jin G, Zhang D, Zhao L, Wang M, Zhu Q, Zhu L, Sun Y, Liu X, Chen X (2019) Natural silibinin modulates amyloid precursor protein processing and amyloid-β protein clearance in APP/PS1 mice. J Physiol Sci 69(4):643–652

Banfi C, Baetta R, Gianazza E, Tremoli E (2017) Technological advances and proteomic applications in drug discovery and target deconvolution: identification of the pleiotropic effects of statins. Drug Discov Today 22(6):848–869

Bhat A, Dalvi H, Jain H, Rangaraj N, Singh SB, Srivastava S (2021) Perspective insights of repurposing the pleiotropic efficacy of statins in neurodegenerative disorders: an expository appraisal. Current Research in Pharmacology and Drug Discovery 2:100012

Borah A, Paul R, Choudhury S, Choudhury A, Bhuyan B, Das Talukdar A, Dutta Choudhury M, Mohanakumar KP (2013) Neuroprotective potential of silymarin against CNS disorders: insight into the pathways and molecular mechanisms of action. CNS Neurosci Ther 19(11):847–853

Cai Z, Qiao PF, Wan CQ, Cai M, Zhou NK, Li Q (2018) Role of blood-brain barrier in Alzheimer's disease. J Alzheimers Dis 63(4):1223–1234. https://doi.org/10.3233/jad-180098

Chiu C, Miller MC, Monahan R, Osgood DP, Stopa EG, Silverberg GD (2015) P-glycoprotein expression and amyloid accumulation in human aging and Alzheimer's disease: preliminary observations. Neurobiol Aging 36(9):2475–2482

Cui H, Su S, Cao Y, Ma C, Qiu W (2021) The altered anatomical distribution of ACE2 in the brain with Alzheimer's disease pathology. Front Cell Dev Biol 9:1581

Cui L, Cai Y, Cheng W, Liu G, Zhao J, Cao H, Tao H, Wang Y, Yin M, Liu T (2017) A novel, multi-target natural drug candidate, matrine, improves cognitive deficits in Alzheimer's disease transgenic mice by inhibiting Aβ aggregation and blocking the RAGE/Aβ axis. Mol Neurobiol 54(3):1939–1952

Dahlin JL, Nissink JWM, Strasser JM, Francis S, Higgins L, Zhou H, Zhang Z, Walters MA (2015) PAINS in the assay: chemical mechanisms of assay interference and promiscuous enzymatic inhibition observed during a sulfhydryl-scavenging HTS. J Med Chem 58(5):2091–2113

Davis R, Reveles KR, Ali SK, Mortensen EM, Frei CR, Mansi I (2015) Statins and male sexual health: a retrospective cohort analysis. J Sex Med 12(1):158–167

Dege N, Gökce H, Doğan OE, Alpaslan G, Ağar T, Muthu S, Sert Y (2022) Quantum computational, spectroscopic investigations on N-(2-((2-chloro-4, 5-dicyanophenyl) amino) ethyl)-4-methylbenzenesulfonamide by DFT/TD-DFT with different solvents, molecular docking and drug-likeness researches. Colloids Surf A 638:128311

Duan S, Guan X, Lin R, Liu X, Yan Y, Lin R, Zhang T, Chen X, Huang J, Sun X (2015) Silibinin inhibits acetylcholinesterase activity and amyloid β peptide aggregation: a dual-target drug for the treatment of Alzheimer's disease. Neurobiol Aging 36(5):1792–1807

Gökce H, Şen F, Sert Y, Abdel-Wahab BF, Kariuki BM, El-Hiti GA (2022) Quantum computational investigation of (E)-1-(4-methoxyphenyl)-5-methyl-N'-(3-phenoxybenzylidene)-1H-1,2,3-triazole-4-carbohydrazide. Molecules 27(7). https://doi.org/10.3390/molecules27072193

Hampel H, Vassar R, De Strooper B, Hardy J, Willem M, Singh N, Zhou J, Yan R, Vanmechelen E, De Vos A (2021) The β-secretase BACE1 in Alzheimer's disease. Biol Psychiat 89(8):745–756

Huang Y-Y, Fang N, Luo H-R, Gao F, Zou Y, Zhou L-L, Zeng Q-P, Fang S-s, Xiao F, Zheng Q (2020) RP1, a RAGE antagonist peptide, can improve memory impairment and reduce Aβ plaque load in the APP/PS1 mouse model of Alzheimer's disease. Neuropharmacology 180:108304

Humphrey W, Dalke A, Schulten K (1996) VMD: visual molecular dynamics. J Mol Graph 14(1):33–38

Husain I, Akhtar M, Abdin MZ, Islamuddin M, Shaharyar M, Najmi A (2018) Rosuvastatin ameliorates cognitive impairment in rats fed with high-salt and cholesterol diet via inhibiting acetylcholinesterase activity and amyloid beta peptide aggregation. Hum Exp Toxicol 37(4):399–411

Husain I, Akhtar M, Vohora D, Abdin MZ, Islamuddin M, Najmi AK (2017) Rosuvastatin attenuates high-salt and cholesterol diet induced neuroinflammation and cognitive impairment via preventing nuclear factor KappaB pathway. Neurochem Res 42(8):2404–2416

Husain I, Khan S, Khan S, Madaan T, Kumar S, Najmi AK (2019) Unfolding the pleiotropic facades of rosuvastatin in therapeutic intervention of myriads of neurodegenerative disorders. Clin Exp Pharmacol Physiol 46(4):283–291

Jagadeb M, Rath SN, Sonawane A (2019) In silico discovery of potential drug molecules to improve the treatment of isoniazid-resistant Mycobacterium tuberculosis. J Biomol Struct Dyn 37(13):3388–3398. https://doi.org/10.1080/07391102.2018.1515116

Jin L, Liu C, Zhang N, Zhang R, Yan M, Bhunia A, Zhang Q, Liu M, Han J, Siebert H-C (2021) Attenuation of human lysozyme amyloid fibrillation by ACE inhibitor captopril: a combined spectroscopy, microscopy, cytotoxicity, and docking study. Biomacromol 22(5):1910–1920

Jin P, Pan Y, Pan Z, Xu J, Lin M, Sun Z, Chen M, Xu M (2018) Alzheimer-like brain metabolic and structural features in cholesterol-fed rabbit detected by magnetic resonance imaging. Lipids Health Dis 17(1):61. https://doi.org/10.1186/s12944-018-0705-9

Jo S, Kim T, Iyer VG, Im W (2008) CHARMM-GUI: a web-based graphical user interface for CHARMM. J Comput Chem 29(11):1859–1865

Kim S, Lee J, Jo S, Brooks III CL, Lee HS, Im W (2017) CHARMM-GUI ligand reader and modeler for CHARMM force field generation of small molecules. In: Wiley Online Library

Knapp B, Lederer N, Omasits U, Schreiner W (2010) vmdICE: a plug-in for rapid evaluation of molecular dynamics simulations using VMD. J Comput Chem 31(16):2868–2873

Laskowski RA, Swindells MB (2011) LigPlot+: multiple ligand–protein interaction diagrams for drug discovery. In: ACS Publications

Le D, Brown L, Malik K, Murakami S (2021) Two opposing functions of angiotensin-converting enzyme (ACE) that links hypertension, dementia, and aging. Int J Mol Sci 22(24):13178

Lee J-S, Kim ES, Lee HG (2017) Improving the water solubility and antimicrobial activity of silymarin by nanoencapsulation. Colloids Surf B 154:171–177

Liu H, Hou T (2016) CaFE: a tool for binding affinity prediction using end-point free energy methods. Bioinformatics 32(14):2216–2218

Lütjohann D, Meichsner S, Pettersson H (2012) Lipids in Alzheimer's disease and their potential for therapy. Clin Lipidol 7(1):65–78

Malathi K, Anbarasu A, Ramaiah S (2019) Identification of potential inhibitors for Klebsiella pneumoniae carbapenemase-3: a molecular docking and dynamics study. J Biomol Struct Dyn 37(17):4601–4613. https://doi.org/10.1080/07391102.2018.1556737

Mawuenyega KG, Sigurdson W, Ovod V, Munsell L, Kasten T, Morris JC, Yarasheski KE, Bateman RJ (2010) Decreased clearance of CNS β-amyloid in Alzheimer's disease. Science 330(6012):1774–1774

Mirzaei N, Davis N, Chau TW, Sastre M (2022) Astrocyte reactivity in Alzheimer's disease: therapeutic opportunities to promote repair. Curr Alzheimer Res 19(1):1–15

Mohamed LA, Keller JN, Kaddoumi A (2016) Role of P-glycoprotein in mediating rivastigmine effect on amyloid-β brain load and related pathology in Alzheimer's disease mouse model. Biochim Biophys Acta Mol Basis Dis 1862(4):778–787

Mori T, Paris D, Town T, Rojiani AM, Sparks DL, Delledonne A, Crawford F, Abdullah LI, Humphrey JA, Dickson DW (2001) Cholesterol accumulates in senile plaques of Alzheimer disease patients and in transgenic APPsw mice. J Neuropathol Exp Neurol 60(8):778–785

Morris GM, Huey R, Lindstrom W, Sanner MF, Belew RK, Goodsell DS, Olson AJ (2009) AutoDock4 and AutoDockTools4: automated docking with selective receptor flexibility. J Comput Chem 30(16):2785–2791

O'Boyle NM, Banck M, James CA, Morley C, Vandermeersch T, Hutchison GR (2011) Open Babel: an open chemical toolbox. J Cheminformatics 3(1):1–14

Omolaoye TS, Halabi MO, Mubarak M, Cyril AC, Duvuru R, Radhakrishnan R, Du Plessis SS (2022) Statins and male fertility: is there a cause for concern? Toxics 10(10):627

Pasieka A, Panek D, Szałaj N, Espargaró A, Więckowska A, Malawska B, Sabaté R, Bajda M (2021) Dual inhibitors of amyloid-β and tau aggregation with amyloid-β disaggregating properties: extended in cellulo, in silico, and kinetic studies of multifunctional anti-Alzheimer's agents. ACS Chem Neurosci 12(11):2057–2068

Phillips JC, Hardy DJ, Maia JD, Stone JE, Ribeiro JV, Bernardi RC, Buch R, Fiorin G, Hénin J, Jiang W (2020) Scalable molecular dynamics on CPU and GPU architectures with NAMD. J Chem Phys 153(4):044130

Pires DE, Blundell TL, Ascher DB (2015) pkCSM: predicting small-molecule pharmacokinetic and toxicity properties using graph-based signatures. J Med Chem 58(9):4066–4072

Porwal O, Ameen MSM, Anwer ET, Uthirapathy S, Ahamad J, Tahsin A (2019) Silybum marianum (milk thistle): review on Its chemistry, morphology, ethno medical uses, phytochemistry and pharmacological activities. J Drug Deliv Ther 9(5):199–206

Rauf A, Imran M, Khan IA, ur-Rehman M, Gilani SA, Mehmood Z, Mubarak MS (2018) Anticancer potential of quercetin: a comprehensive review. Phytother Res 32(11):2109–2130

Reyes-Farias M, Carrasco-Pozo C (2019) The anti-cancer effect of quercetin: molecular implications in cancer metabolism. Int J Mol Sci 20(13):3177

Sadeghi M, Sabbaghziarani F, Soleimani P, Ashtarimajelan MR, Zafari F (2021) Association of atorvastatin with increased growth and quality of immature mouse oocytes in-vitro. Sci J Kurdistan Univ Medical Sci 26(4):30–37

Sander T (2001) OSIRIS property explorer. Organic Chemistry Portal

Sanner MF (1999) Python: a programming language for software integration and development. J Mol Graph Model 17(1):57–61

Schramm S, Gunesch S, Lang F, Saedtler M, Meinel L, Högger P, Decker M (2018) Investigations into neuroprotectivity, stability, and water solubility of 7-O-cinnamoylsilibinin, its hemisuccinate and dehydro derivatives. Arch Pharm 351(11):1800206

Shafabakhsh R, Asemi Z (2019) Quercetin: a natural compound for ovarian cancer treatment. J Ovarian Res 12(1):1–9

Shannon P, Markiel A, Ozier O, Baliga NS, Wang JT, Ramage D, Amin N, Schwikowski B, Ideker T (2003) Cytoscape: a software environment for integrated models of biomolecular interaction networks. Genome Res 13(11):2498–2504. https://doi.org/10.1101/gr.1239303

Shinohara M, Tachibana M, Kanekiyo T, Bu G (2017) Role of LRP1 in the pathogenesis of Alzheimer's disease: evidence from clinical and preclinical studies: thematic review series: ApoE and lipid homeostasis in Alzheimer's disease. J Lipid Res 58(7):1267–1281

Shiri F, Pirhadi S, Ghasemi JB (2019) Dynamic structure based pharmacophore modeling of the acetylcholinesterase reveals several potential inhibitors. J Biomol Struct Dyn 37(7):1800–1812. https://doi.org/10.1080/07391102.2018.1468281

Singh A, Kumar A, Verma RK, Shukla R (2020) Silymarin encapsulated nanoliquid crystals for improved activity against beta amyloid induced cytotoxicity. Int J Biol Macromol 149:1198–1206

Singh H, Agrawal DK (2022) Therapeutic potential of targeting the receptor for advanced glycation end products (RAGE) by small molecule inhibitors. Drug Dev Res 83(6):1257–1269

Soleimani V, Delghandi PS, Moallem SA, Karimi G (2019) Safety and toxicity of silymarin, the major constituent of milk thistle extract: an updated review. Phytother Res 33(6):1627–1638. https://doi.org/10.1002/ptr.6361

Szklarczyk D, Franceschini A, Wyder S, Forslund K, Heller D, Huerta-Cepas J, Simonovic M, Roth A, Santos A, Tsafou KP, Kuhn M, Bork P, Jensen LJ, von Mering C (2015) STRING v10: protein-protein interaction networks, integrated over the tree of life. Nucleic Acids Res 43:D447-452. https://doi.org/10.1093/nar/gku1003

Tang S-M, Deng X-T, Zhou J, Li Q-P, Ge X-X, Miao L (2020) Pharmacological basis and new insights of quercetin action in respect to its anti-cancer effects. Biomed Pharmacother 121:109604

Tijms BM, Vermunt L, Zwan MD, van Harten AC, van der Flier WM, Teunissen CE, Scheltens P, Visser PJ, ADNI, (2018) Pre-amyloid stage of Alzheimer's disease in cognitively normal individuals. Ann Clin Transl Neurol 5(9):1037–1047

Tolstova AP, Adzhubei AA, Mitkevich VA, Petrushanko IY, Makarov AA (2022) Docking and molecular dynamics-based identification of interaction between various beta-amyloid isoforms and RAGE receptor. Int J Mol Sci 23(19):11816

Toth PP, Dayspring TD (2011) Drug safety evaluation of rosuvastatin. Expert Opin Drug Saf 10(6):969–986

Trott O, Olson AJ (2010) AutoDock Vina: improving the speed and accuracy of docking with a new scoring function, efficient optimization, and multithreading. J Comput Chem 31(2):455–461

Tvrdý V, Pourová J, Jirkovský E, Křen V, Valentová K, Mladěnka P (2021) Systematic review of pharmacokinetics and potential pharmacokinetic interactions of flavonolignans from silymarin. Med Res Rev 41(4):2195–2246. https://doi.org/10.1002/med.21791

Urina-Jassir M, Pacheco-Paez T, Paez-Canro C, Urina-Triana M (2021) Statin associated adverse reactions in Latin America: a scoping review. BMJ Open 11(10):e050675

Vuorio A, Kovanen PT, Raal F (2022) Cholesterol-lowering drugs for high-risk hypercholesterolemia patients with COVID-19 while on Paxlovid™ therapy. Future Virol. https://doi.org/10.2217/fvl-2022-0060

Wolozin B (2011) Statins and therapy of Alzheimer's disease: questions of efficacy versus trial design. Alzheimers Res Ther 3(6):1–3

Yang W, Shi H, Zhang J, Shen Z, Zhou G, Hu M (2017) Effects of the duration of hyperlipidemia on cerebral lipids, vessels and neurons in rats. Lipids Health Dis 16(1):26. https://doi.org/10.1186/s12944-016-0401-6

Yue Q, Song Y, Liu Z, Zhang L, Yang L, Li J (2022) Receptor for advanced glycation end products (RAGE): a pivotal hub in immune diseases. Molecules 27(15):4922